NASA
Technical
Paper
2038

August 1982

Studies of Implicit and Explicit Solution Techniques in Transient Thermal Analysis of Structures

Howard M. Adelman,
Raphael T. Haftka,
and James C. Robinson

NASA

SUMMARY

This paper discusses a research effort directed toward increased efficiency in calculating transient temperature fields in complex aerospace vehicle structures. Explicit solution techniques which require minimal computation per time step and implicit techniques which permit larger time steps because of better stability are reviewed and evaluated. A set of implicit solution algorithms with variable time steps (GEARIB) is described and evaluated. Test problems for evaluating the algorithms include a coarse model of the Space Shuttle Orbiter wing, an insulated frame test article, a metallic panel for a thermal protection system, and detailed models of single-bay and three-bay sections of the Shuttle wing. Results generally indicate that implicit algorithms, especially GEARIB with variable step size and order, are faster than explicit algorithms for transient structural heat-transfer problems when the governing equations are stiff. Stiff equations occur in many practical problems particularly in insulated thin metal structures.

The effect on algorithm performance of different models of an insulated cylinder was also studied. The study revealed that the stiffness of the problem is highly sensitive to modeling details and that careful modeling can reduce the stiffness of the resulting equations to the extent that explicit methods may be advantageous.

Studies of partitioning techniques for improving the performance of solution algorithms were carried out. A mixed implicit-explicit technique developed for dynamic response has been adapted to thermal problems and is demonstrated. In this method, the model is separated into stiff and nonstiff regions. The implicit algorithm is applied to the stiff portion and the explicit to the nonstiff portion. Two operator-splitting techniques for speeding up the solution of the algebraic equations associated with implicit algorithms are also described and demonstrated. Both are based on separating the coefficient matrices into two parts and solving the resulting equations by iteration. The first technique bases the separation on stiff and nonstiff elements of the structure, and the second bases the separation on the sparsity structure of the matrix. The most effective of the techniques tried was a separation based on matrix sparsity (using an incomplete Cholesky decomposition) combined with conjugate gradient iteration. Especially noteworthy is the fact that the performance of this technique is insensitive to the band structure of the matrix.

INTRODUCTION

An effort is in progress at the Langley Research Center to gain increased efficiency in the prediction and optimization of the thermal-structural behavior of aerospace vehicle structures. A principal task is to reduce the computing effort for obtaining transient temperatures. This paper is focused on (1) assessment of the performance of explicit and implicit temporal integration algorithms, (2) the effects of modeling on the performance of the algorithms, and (3) techniques for solving the algebraic equations associated with implicit methods.

In the current and recent literature, many of the difficulties associated with the solution of transient heat-transfer problems and other time-dependent physical

problems are associated with the stiff[1] nature of the governing differential equations (refs. 1 to 7). Stiff sets of equations for thermal applications occur in problems where the rate of heating is significantly slower than the speed of propagation of temperature differences between adjacent points in the model. In particular, insulated thin metal structures under long-duration heating often lead to stiff equations. A preference is evident among researchers for implicit algorithms for solution of stiff sets of ordinary differential equations. However, many engineering analysts prefer to use the longer established explicit algorithms, even for stiff problems. A partial explanation for this dichotomy is that the full power of the implicit approach has not been transferred from researchers to engineering analysts. In particular, implicit algorithms are usually implemented in computer programs with a fixed time step (refs. 8 to 10).

In the explicit algorithms, the time step is limited (often severely) in order for the technique to be stable. In the implicit algorithms, there is no stability-imposed limitation on step size, and the step size is limited by solution accuracy only. This conclusion holds in general for linear systems, but it is also found to hold in many nonlinear applications (ref. 11). Thus implicit algorithms can, in general, use much larger time steps than explicit algorithms; this is especially true for stiff problems. Because a single explicit time step is computationally faster than a single implicit time step, the key to the advantageous use of implicit algorithms is to use the largest possible time step size.

The strategy advocated for the solution of problems by implicit methods is to use algorithms with variable step size and order and to automatically select both throughout the solution process (refs. 12 to 15). A promising set of algorithms, developed to implement this strategy, is denoted the GEAR algorithms (refs. 13 and 14). A version of the GEAR algorithms well-suited to heat-transfer analysis, denoted GEARIB, has been recently installed in the SPAR finite-element thermal analyzer (ref. 8) for testing. Early evaluations of GEARIB in SPAR and comparisons with other implicit algorithms were described in reference 16 for the first three problems in this paper.

The first objective of the present paper is to describe recent evaluations, improvements, and demonstrations in the use of explicit and implicit algorithms for transient thermal analysis of structures. A coarse model of the Space Shuttle Orbiter wing, an insulated frame test article, a metallic multiwall thermal protection system panel, and detailed models of single-bay and three-bay sections of the Shuttle wing are analyzed. Comparisons between implicit and explicit algorithms are presented and the performance of the GEARIB algorithms, especially the value of variable step size, is demonstrated.

A characteristic of thermal analysis by finite-element and lumped-parameter techniques is that modeling strongly affects the stiffness. Since stiffness is one of the key factors in the performance of implicit and explicit algorithms, the second objective of the paper is to study the effects of modeling. This paper describes a study carried out for an insulated cylinder of the effects of modeling on the performance of explicit and implicit algorithms.

---

[1]Stiff sets of ordinary differential equations are characterized by solutions with widely varying time constants. The typical case is when the solution to the homogeneous problem has some very small time constants compared with those of the forcing function (ref. 1).

Finally, when the stiffness of the problem is due to only part of the finite-element model, partitioning techniques may be useful. The third objective of the paper is to explore the potential of some partitioning techniques. The first is a mixed implicit-explicit algorithm developed by Hughes and Liu (refs. 17 and 18) which was adapted to thermal analysis in reference 19 and is demonstrated for an insulated panel. Also, two techniques for speeding up the solution of the algebraic equations associated with implicit algorithms are described and demonstrated. Both are based on separating the coefficient matrices into two parts and solving the resulting equations by iteration. The first technique bases the separation on stiff and nonstiff elements of the structure and the second bases the separation on the sparsity structure of the matrix (ref. 20).

SYMBOLS

C	capacitance matrix
c_p	heat capacity
DT	integration time step size in SPAR program (ref. 8)
F	right-hand side of equations for transient temperature
h_n	nth time step
K	conductivity matrix
k	thermal conductivity
Q	thermal load vector
R	residual of system of equations generated by implicit method
T	vector of temperatures; dot over T indicates differentiation with respect to time
t	time
t_Q	typical time constant of applied heat loads
t_n	nth time point
t_s	stability limit of time step for explicit algorithms
α	thermal diffusivity
α_i	coefficients in backward-difference method (eq. (6))
β_i	coefficients in backward-difference and Adams-Moulton methods (eqs. (5) and (6))
ρ	mass density

Subscript:

n time step number

NATURE OF ALGORITHMS USED IN TRANSIENT STRUCTURAL THERMAL ANALYSIS

The governing semi-discrete equations for a transient heat-transfer problem discretized by a finite-element or finite-difference technique are as follows:

$$C\dot{T} = Q(T,t) - K(T,t)\,T = F(T,t) \qquad (T(0) = T_o) \tag{1}$$

where T is a vector of temperatures, C and K are matrices, Q and F are vectors, and F is generally a nonlinear function of T. Obtaining an analytical solution to equation (1) is usually impractical and numerical integration methods are used. The simplest numerical integration technique is the Euler method which uses the first two terms in a Taylor series to predict T

$$T(t_{n+1}) = T(t_n) + h_n \dot{T}(t_n) = T(t_n) + h_n C^{-1} F\left[T(t_n),t_n\right] \tag{2}$$

where h_n is the time step size at the nth step. Euler's method is an example of an explicit integration technique, so-named because $T(t_{n+1})$ is given explicitly in terms of known quantities. Another approach to the numerical integration of equation (1) is the backward-difference method which is an example of an implicit method. In this approach,

$$T(t_{n+1}) = T(t_n) + h_n \dot{T}(t_{n+1}) = T(t_n) + h_n C^{-1} F\left[T(t_{n+1}),t_{n+1}\right] \tag{3}$$

Equation (3) is a system of implicit equations for $T(t_{n+1})$, which is generally nonlinear. The explicit algorithm is therefore easier to implement; but, the time step must be bounded to avoid numerical instability (unbounded propagation of numerical errors during the solution). Implicit techniques are generally unconditionally stable for linear systems (and some nonlinear applications) and thus can take larger time steps which are determined from accuracy considerations rather than stability.

For one-dimensional conduction problems, the time for a temperature disturbance to propagate from one point to another is roughly proportional to L^2/α, where L is the distance between the two points and α is the thermal diffusivity. The time step t_s required to insure stability of an explicit integration method is proportional to this intrinsic time. For a finite-element discretization, the explicit time step is determined by the element with the smallest value of L^2/α, where L is the length of the element. The rapidity of variation of the temperature, on the other hand, depends on the time scale of the applied heating. Accuracy considerations require a time step which is comparable to a typical time constant of the applied heat loads t_Q. By definition, a problem is stiff whenever t_Q is much larger than t_s. Implicit methods (in which time steps are bounded only by accuracy requirements) can use large time steps (of order t_Q), whereas explicit methods

which are bound by stability requirements require small time steps (of order L^2/α). It follows that stiff problems are usually best solved by implicit methods. The effort involved in solving a system such as equation (3) is usually cost-effective if a small number of large time steps are used. The preceding comments hold for general transient thermal problems except that the intrinsic time steps have more complex forms than L^2/α.

The Euler method and the backward-difference methods are presented as examples from a large class of explicit and implicit techniques, respectively. Higher order methods (e.g., multistep) in both the explicit and implicit classes typically use more previous information to predict the temperature but the stability properties of explicit multistep methods are similar to those of the Euler method (ref. 11). Explicit methods are unstable for time steps much larger than the smallest value of L^2/α. Accordingly, thermal analysis computer programs generally select explicit time steps automatically based on the stability requirement. When using implicit methods, the analyst is left to select the implicit time step and order without a great deal of guideline information, and often several trial runs are needed. There is an emerging consensus that the preferred approach for integrating stiff systems of ordinary differential equations is to use implicit methods which automatically select the order and the step size based on desired accuracy. One software package, denoted the GEARIB algorithms, has these features and is discussed subsequently.

THE GEARIB ALGORITHMS

Several software packages based on the work of Gear have been developed for general use (ref. 13). The package most appropriate for application to finite-element thermal analysis is denoted GEARIB. This package is intended to solve systems of ordinary differential equations of the form

$$C\dot{T} = F(T,t) \tag{4}$$

The package employs two classes of implicit multistep methods, Adams-Moulton and general backward differences. For nonstiff equations the Adams-Moulton method of orders 1 through 12 is used. This method has the general form

$$T(t_{n+1}) = T(t_n) + h_n \sum_{i=0}^{q} \beta_i \dot{T}(t_{n+1-i}) \tag{5}$$

where q is the order. For stiff equations, backward-difference algorithms of orders 1 through 5 are used. These have the general form

$$T(t_{n+1}) = h_n \beta_0 \dot{T}(t_{n+1}) + \sum_{i=1}^{q} \alpha_i T(t_{n+1-i}) \tag{6}$$

The coefficients α_i and β_i are given in reference 15. GEARIB employs a predictor-corrector approach where equation (5) or (6) is the corrector equation and extrapolation is used for the predictor. The user selects the class of methods (Adams-Moulton or backward differences) and error tolerance. GEARIB automatically selects the step size and order by a technique described in reference 13. The

essence of the step size and order selection technique is that at each time step the error tolerance is compared with an estimate of the actual error resulting from use of the previous step size and order. Both are scaled to force the actual error to be no larger than the specified error tolerance.

Use of the GEARIB algorithms is illustrated by using the backward-difference option (eq. (6)). Applied to equation (4), equation (6) gives

$$R = C\left[T(t_{n+1}) - \sum_{i=1}^{q} \alpha_i \, T(t_{n+1-i})\right] - h_n \beta_0 \, F\left[T(t_{n+1}), t_{n+1}\right] = 0 \tag{7}$$

This system of nonlinear algebraic equations is solved by the modified Newton method; that is,

$$T^{i+1}(t_{n+1}) = T^{i}(t_{n+1}) - \left[\frac{\partial R}{\partial T}\right]^{-1} R \tag{8}$$

where

$$\frac{\partial R}{\partial T} = C - \beta_0 h_n J$$

and $J = \partial F/\partial T$ is the Jacobian of the system. Methods and options used in GEARIB for computing J are described in references 13 and 21.

DESCRIPTION OF TEST PROBLEMS AND RESULTS

As discussed previously, the stiffness of a transient thermal analysis problem is in part dependent on the size of the finite elements used in the modeling. For the same heat loads, a detailed model which has small finite elements will be stiffer than a coarse model which has larger elements. In assessing the performance of explicit and implicit algorithms, it is important to include examples which span the range of model fineness used in practical applications. The test problems were chosen with this in mind. The Space Shuttle Orbiter wing model represents a coarse model suitable for overall trends in early Shuttle thermal analyses. The multiwall thermal protection system panel represents, probably, the most refined model that would be used. The other three examples represent typical models which are somewhere in between the aforementioned two extremes.

In comparing the efficiency of the different algorithms, the Euler method was used as the only explicit method, whereas the first-order backward-difference, the Crank-Nicholson, and the GEARIB algorithms were used to represent implicit methods. Euler was chosen because, of all the power series explicit algorithms available in SPAR, the Euler algorithm (based on the first two terms of the power series) is the most efficient for stability-limited problems. The stability limit for the time step in SPAR is estimated as $t_s = \min (c_{ii}/k_{ii})_i$ where c_{ii} and k_{ii} are the diagonal terms of the capacitance and conductance matrices, respectively. The conductance matrix includes radiation effects. The actual time step used in the analysis was selected to be 95 percent of the estimated stability limit, unless otherwise noted.

Solution times reported in comparing the algorithms are central processor unit (CPU) times. (A comparison of solution times for all five examples is presented in table 1.) All calculations were performed on the Control Data CYBER 173 computer system at the Langley Research Center under network operating systems (NOS) 1.3 and 1.4 unless otherwise noted. It is recognized that the use of GEARIB to represent implicit algorithms and the Euler method to represent explicit algorithms is somewhat biased. However, for stability-limited parabolic problems such as the stiff thermal analysis problems herein, the use of more advanced explicit algorithms are not expected to be significantly more efficient than the Euler method. Thus, the bias is probably not very significant.

Space Shuttle Orbiter Wing

The Space Shuttle Orbiter wing (fig. 1(a)) was chosen as the first example problem. The SPAR finite-element model (fig. 1(b)) consists of a relatively coarse idealization of the structure augmented by a representation of the insulation attached to the upper and lower surfaces. This model is useful for obtaining rough overall qualitative ideas about the temperature distributions but is too coarse for a detailed thermal analysis. The structure is modeled by one-dimensional, triangular, and quadrilateral (K21, K31, and K41, respectively) SPAR conduction elements. The insulation on each surface is modeled by six layers of one-dimensional conduction elements. Use of these latter elements neglects lateral heat transfer in the insulation. This modeling decision was guided by results from a previous wing model (ref. 21) in which lateral heat transfer in the insulation was included. It was found that lateral temperature gradients were negligible when compared with gradients through the insulation. The complete model contains 2289 grid points, 840 one-dimensional (1-D) and 560 two-dimensional (2-D) elements in the structure, and 1962 one-dimensional elements in the insulation. Thermal properties of the aluminum structure are temperature dependent; thermal properties of the insulation are temperature and pressure dependent. The pressure dependence is treated in SPAR as time dependence using the variation of pressure as a function of time from the trajectory data for a simulated flight. As a result of these dependencies, the conductivity of the insulation in the outer layers changes by a factor of nine during the temperature history.

For the purpose of this analysis, the heating on the wing is represented by a specified temperature history on the external surface of the insulation on the under side of the wing (shown as the solid line in fig. 2) and is roughly indicative of atmospheric reentry heating. Temperature histories of the wing for 4500 seconds were computed by using the explicit (Euler), implicit (Crank-Nicholson), and GEARIB algorithms. Figure 2 shows the temperature histories of a point in the structure and a point in the insulation at a typical wing cross section. The explicit, implicit, and GEARIB algorithms produced essentially the same temperature histories. Solution time comparisons are shown in table 1(a) along with the time steps used to obtain comparable accuracy. The explicit algorithm used a time step of 10 seconds - in fact, the stability limit calculated by SPAR (t_s) was over 100 seconds but the time step size was dictated by accuracy and the need to periodically update temperature-dependent material properties. The large permitted time step is due to the coarse modeling of the structure which did not include any thin, high-conducting, or radiating elements which can lead to stiff equations. The implicit algorithm (Crank-Nicholson) required a time step of 10 seconds to achieve comparable accuracy and required about five times as much computer time as the explicit algorithm. The GEARIB algorithms performed very well for this problem. By adaptively varying the time step from 1.0 second early in the temperature history to as large as 528 seconds toward the

end, GEARIB required only 570 CPU seconds to complete the solution. GEARIB required only eight recalculations and refactorings of the Jacobian, which shows that even with the large variations in material properties, the problem is only mildly nonlinear.

Insulated Frame Test Article

An insulated frame test article analyzed and tested under transient heating as described in reference 22 is shown in figure 3(a). The test article consisted of an aluminum skin/stringer structure with two corrugated aluminum frames. An installation of FRSI (flexible reusable surface insulation) was placed on the skin surface. The test article was also equipped with an auxiliary insulation blanket to prevent direct heating of the test article sides and back. The principal purpose of the study of the configuration, as discussed in reference 22, was to evaluate the thermal performance of Shuttle FRSI during a simulated flight. A secondary purpose was to evaluate by comparison with test data the adequacy of thermal analysis techniques needed by the Shuttle contractors for preflight thermal and thermal stress analysis.

Because of symmetry, the lumped-parameter model from reference 22 (not shown in the figure) consisted of a two-dimensional section of half the structure. The lumped-parameter model was converted to a finite-element model for analysis with SPAR. The SPAR finite-element model (fig. 3(b)) contains 149 grid points and 148 elements including one-dimensional elements which account for conduction in the aluminum structure and radiation across the air gap and two-dimensional elements which model conduction in the insulation and across the gap. Minor modifications were made to the finite-element model following the conversion from the lumped-parameter model. These modifications consisted of eliminating or consolidating some extremely thin or short finite elements in the aluminum structure in order to reduce the stiffness of the equations and to increase the allowable time step for the explicit solution algorithm. The properties of the aluminum structure are functions of temperature, and, as in the previous example, the properties of the insulation are functions of temperature and pressure. The heating is simulated by a temperature history at the outer surface of the insulation.

The temperature history for the frame was computed by using the explicit (Euler) and implicit techniques (Crank-Nicholson and backward differences) and GEARIB. Comparisons of solution times are given in table 1(b). The explicit algorithm had a stability limit t_s of 0.16 second and required 1723 seconds. This time step was controlled by conduction through the aluminum elements along the center and front of the model. The solution times using the Crank-Nicholson algorithm varied from 475 to 65 seconds corresponding to variations in the time step from 1.0 and 50 seconds. The solution times for backward differences were essentially the same as those of Crank-Nicholson and are not shown. The GEARIB algorithm used time steps from 50 to 170 seconds and the solution time was 54 seconds. As indicated in table 2, there is very little loss of accuracy in either the structure or insulation temperatures with increased time-step size.

The accuracy of the solutions obtained by the various techniques is further assessed in figure 4 which displays temperature histories at a point in the outer layer of the aluminum structure corresponding to node 309. (See fig. 3.) The solid curve in figure 4 represents specified temperatures at the outer surface of the insulation (node 29). The dashed line shows temperatures obtained by the SPAR analyses which are plotted as a single curve since there is little difference between the results. The long-dash—short-dash curve shows analytical results from the lumped-

parameter analysis of reference 22, which are also in close agreement with the SPAR temperatures. The circles in figure 4 represent test data from reference 22. The close agreement between the numerical and experimental results indicates that the models are adequate to simulate the temperature history in the test article.

Multiwall Thermal Protection System Panel

The next example problem is one which evolved out of a study of the thermal performance of a titanium multiwall thermal protection system (TPS) panel which is under study for future use on space transportation systems (ref. 23). A high level of modeling detail was required to accurately represent the local thermal conductivity of the multiwall concept and to assess some approximations used in the work reported in reference 23. The configuration, depicted in figure 5(a), consists of alternating layers of flat and dimpled sheets fused at the crests of the dimpled sheets to form a sandwich. The representation of a typical dimpled sheet is shown in figure 5(b). For the purpose of this analysis, it is assumed that the heating does not vary laterally. This assumption, in addition to the regular geometry of the structure, leads to the modeling simplification wherein only a triangular prismatic section (indicated in fig. 5(a)) of the panel needs to be modeled. The intersection of this prism with a typical dimpled layer is indicated by the shaded triangle in figure 5(b).

The finite-element model shown in figure 5(c) contains 333 grid points located on nine titanium sheets (five horizontal and four inclined). The model contains 288 triangular and quadrilateral metal conduction elements, 264 solid elements (K61 and K81) which account for air conduction between the layers, and 544 triangular and quadrilateral radiation elements which account for radiation heat transfer between adjacent horizontal and inclined sheets. Thermal properties of titanium and air are functions of temperature. Radiation exchange (view) factors were computed and supplied to SPAR with the TRASYS II computer program (ref. 24).

The temperature history in the panel resulting from a specified transient temperature at the outer surface of the panel was computed for 3200 seconds. Results were obtained with SPAR by using explicit, Crank-Nicholson, backward-difference, and GEARIB algorithms. Solution time comparisons are presented in table 1(c). The explicit algorithm had a stability-limited time step t_s of 0.007 second. This time step was dictated by the short conduction paths between the vertices of adjacent triangular layers. The small time step indicates that this is an extremely stiff problem as may be expected because of the fine detail in modeling. Required solution time for the explicit algorithm was estimated by extrapolation to be 98 400 seconds.

The Crank-Nicholson solution was carried out with time steps of 1.0 and 5 seconds, which led to solution times of 28 400 (estimation based on extrapolation) and 6352 seconds, respectively. Backward difference was used with the same time steps and had the same solution times. GEARIB took time steps ranging between 1.0 and 113 seconds and required a solution time of 2754 seconds. A plot of typical temperature histories for a point midway through the panel and the primary structure are shown in figure 6 along with the applied outer surface temperature. The results shown are from the implicit algorithm with a time step of 5 seconds and are identical to results with a time step of 1 second and GEARIB.

Three Bays of Shuttle Wing

A three-bay section of the Shuttle wing (fig. 7) was analyzed by the authors of reference 25 and the model was made available for the present study. The finite-element model shown in figure 8 for wing station 328, unlike the coarse model of the complete wing shown previously, is typical of the level of detail used in Shuttle thermal modeling practice. The purpose of the study described in reference 25 was to use thermal analysis tools to predict temperatures measured during the first Shuttle flight. Temperatures predicted by the SPAR program were found to be in good agreement with flight data. The forward spar web of bay 1 is made of aluminum honeycomb core sandwich plate, and the rest are corrugated plates. The upper and lower skins are hat-stringer stiffened. The lower skin is covered with HRSI (high-temperature reusable surface insulation). The upper skin is covered with LRSI (low-temperature reusable surface insulation) and FRSI.

In order to account for the spanwise heat flow and the effect of the rib trusses, the wing segment was modeled in three dimensions. The finite-element model has 915 joint locations. The modeling was limited to the major load-carrying portion. The wing skins and spar webs, rib caps, shear webs, insulation surface coatings, and RTV (room temperature vulcanized) adhesive layers lying on both sides of the SIP (strain isolator pad) were modeled with SPAR K41 elements. The spar caps, rib caps, and rib trusses were modeled with SPAR K21 elements. The insulation was modeled in 13 layers on the lower surface and 5 layers on the upper surface with SPAR K81 elements. The SIP was modeled by one layer of SPAR K81 elements. Aerodynamically heated surfaces were modeled with one layer of K41 elements. For the external and internal radiant heat energy exchanges, a layer of SPAR R41 elements (four-node radiation exchange elements) was attached to the outer surface of the insulation and the exposed aluminum surfaces. For the spar webs with two sides exposed (lying between the bays), one layer of R41 elements was used for each exposed surface. Outer surfaces of the forward and rear spar webs were totally insulated. Internal convection and external convective cooling (negligible during entry) were ignored. The heating rates vary along the model from bay to bay. The heating rates used are from reference 25 and are shown in figure 9.

A 3500-second history of temperature for the model was computed by use of the explicit (Euler), implicit (Crank-Nicholson), and GEARIB methods. Solution time comparisons are given in table 1(d). The rather nonstiff nature of this model leads to a relatively large explicit time step t_s of 2.6 seconds. The Crank-Nicholson algorithm required a time step of 5 seconds to obtain comparable accuracy. Not surprisingly, the explicit solution time was significantly less than the Crank-Nicholson solution time. The GEARIB method used time steps varying from 0.1 to 229 seconds for a solution time that is less than one-fifth the time required by the explicit technique and it obtained equal accuracy.

Single Bay of Shuttle Wing

The single-bay model shown in figure 10 represents a two-dimensional section through the wing in the third bay at wing station 240. The model was obtained from the authors of reference 25. The SIP and RTV layers (lying on both sides of the SIP) were modeled with SPAR K41 elements. The spar webs and caps, rib caps, and trusses and skins were modeled with SPAR K21 elements so as to form a frame. The insulation was modeled in 10 layers on the lower surface and 3 layers on the upper surface with SPAR K41 elements. Radiation heat transfer from the upper and lower surfaces and inside the cavity was modeled with R21 elements. The single-bay model contained a

total of 123 grid points and 191 elements. The heat rates as functions of time were obtained from the authors of reference 25 and are shown in figure 11.

A 3500-second temperature history of the model was performed by use of the Euler, Crank-Nicholson, and GEARIB algorithms. Solution time comparisons are given in table 1(e). The model is stiff due to the short heat paths through the aluminum elements near the corner of the frame. The time step needed by the Euler technique t_s was 0.1 second. The Crank-Nicholson method was used with a time step of 1.0 second resulting in a solution time which was one-third that of the Euler technique. With GEARIB, time steps varied from 0.1 second at the beginning of the solution up to 225 seconds toward the end of the solution. The solution time was less than 10 percent of the Euler solution time and less than 25 percent of the Crank-Nicholson solution time.

EFFECT OF MODELING ON ALGORITHM PERFORMANCE

This section gives some insight concerning how modeling details can affect the performance of transient solution algorithms - especially explicit algorithms. The structure chosen for the study is an insulated cylindrical shell shown in figure 12. The cylinder is 720 inches in length and 180 inches in diameter. The aluminum is 0.1 inch thick and the insulation (insul) is 2.0 inches thick. The outer surface of the insulation is heated over a region which consists of one-third the length and one-half the circumference.

Three finite-element models are used in the study. Because of symmetry, only half the cylinder is modeled in each case. In model I, solid (K81) elements are used exclusively - 39 along the cylinder length, 4 around the circumference, and 3 through the depth (2 elements in the insulation and 1 in the structure). The outer surface has quadrilateral elements which receive the heating and radiation elements (R41) which radiate to space. Model I contains 800 grid points and 650 elements. The use of solid elements to model the metal layer is not necessary and was used here as an extreme example of the effect of thin metal elements on stiffness. In model II the solid elements in the metal layer are replaced by quadrilateral elements (K41) in which temperatures do not vary through the thickness; this is generally a good assumption for thin metal structures. Model II has an extra layer of solid elements in the insulation in order to preserve the number of grid points in the model at 800. In model III the grid points are identical to those of model II, but the insulation is modeled with one-dimensional conductors (K21). This model neglects lateral heat conduction but, as mentioned previously in connection with the coarse Shuttle wing model, this effect is small for the class of insulated flight structures of primary interest in the present work.

Another aspect of the effect of modeling is comparison of results from finite-element and lumped-parameter models. To investigate this, the MITAS lumped-parameter computer program (ref. 26) was used to analyze the cylinder. The finite-element model I was converted to a lumped-parameter model by use of the CINGEN program (ref. 27). The resulting lumped-parameter model contained 625 nodes as compared to 800 grid points in the finite-element model. The unknown MITAS temperatures are located only at the centroids of each lump.

The first 2000 seconds of the cylinder temperature response to the heating rate history shown in figure 13 were computed in each model. The explicit (Euler) and implicit (backward-difference) algorithms were used for all models, and GEARIB was used for the SPAR models. Solution times are summarized in table 3. Model I is

extremely stiff as evidenced by the small time step (t_s) of 0.06 second required for stability of the explicit algorithm. The high stiffness is due to the use of K81 elements to model the metal layer. In model II, the stiffness has been essentially eliminated by replacing the three-dimensional elements in the metal layer with two-dimensional elements. In model II, the explicit technique uses time steps ranging from 2.4 to 10 seconds and is faster than backward-difference and GEARIB techniques. In model III, due to low stiffness again, the explicit algorithm is faster than the implicit but GEARIB is slightly faster than the explicit technique.

MITAS computation times are shown in table 3. Because none of the SPAR models is equivalent to the MITAS model in terms of the number of unknown temperature or nodal connections, no direct comparison of MITAS and SPAR solution times are appropriate. The MITAS model is not particularly stiff as evidenced by the large time step used in the explicit solution technique. SPAR models II and III which begin to resemble the MITAS model in certain respects are also less stiff and favor explicit algorithms.

Figure 14 contains temperature histories of a point in the metal portion of the cylinder 45° inside the edge of the heated region and 18 inches from the end of the cylinder. Model II is considered to be the best of the models (recall the additional insulation elements used); thus, the temperatures represented by the dashed line are expected to be the most accurate. These results are bracketed by results from model I and MITAS (from above) and by model III (from below). There are negligible differences between temperatures from the implicit and explicit solutions for any given model. Results from models II and III are different from those of model I because of the extra layer of insulation elements. The MITAS temperature history agrees well with that of model I (on which the MITAS model is based) except for some differences beginning at about 1400 seconds.

Figure 15 contains temperature distributions from each model along a generator of the cylinder 45° from the edge of the heated region which contains both the heated and unheated parts. Temperatures are plotted for the aluminum surface of the cylinder. All four models give consistent results and are able to track the large temperature drop across the boundary between the heated and unheated regions. Of particular note is the close agreement of the results from models II and III. This close agreement tends to verify the adequacy of using one-dimensional conduction elements in the insulation of model III, which led to substantial solution time savings. The results of this modeling study show that modeling can have a major impact on the stiffness of the system and on solution times, especially for an explicit algorithm.

EFFECT OF MATRIX SCALING

For models I and II of the cylinder problem (table 3), the GEARIB algorithm, despite using much larger time steps, was only marginally faster than the Crank-Nicholson implicit algorithm, and for model II it was slower than the explicit method. This is partially due to the different ways of handling the temperature-dependent material properties. In the explicit and implicit methods as implemented in SPAR, the properties are represented as piecewise constant within time intervals specified by the user (by the input quantity TI) in SPAR. Material properties for each element are evaluated at the beginning of each interval based on the average temperature of the element nodes, and the conductivity and capacitance matrices are regenerated only at those times. Results for models I, II, and III in table 3 were obtained by using TI = 20 seconds. For the GEARIB algorithm, the material prop-

erties are assumed to vary continuously and the residual R (eq. (7)) must be evaluated at each iteration used in solving equation (8). Thus, there is a need for continuous regeneration of the conductivity and capacitance matrices. This extra effort is the price paid for higher accuracy. Furthermore, this burden of recalculating matrices and residuals shows up most noticeably in problems which utilize solid (K81) elements because of the size of the matrices for those elements (model III does not contain K81 elements). A way to ease the burden (for thermally isotropic elements) has been identified and has been recently implemented in SPAR. The method is to generate the matrices only once for unit values of the appropriate property and simply scale the matrices by the property whenever it is updated. The effect of scaling on the solution time is shown in table 4. The most significant impact of scaling is in the implicit and GEARIB solution times in models I and II which contain K81 elements and the least impact is seen in model III which has none. Scaling thus helps to ease the burden on implicit algorithms of regeneration of conductivity matrices for the K81 elements and makes them more attractive for use in large complex models. Scaling has a minimal effect on the explicit solution time for model I because most of that time is due to time marching and relatively little is due to matrix regeneration.

PARTITIONING METHODS

The examples in the previous section have shown that stiffness of the problem is the major factor in choosing an explicit or an implicit temporal integration method for thermal analysis. When the problem is stiff, an implicit method is preferable; when the problem is nonstiff, an explicit method is more efficient. Some problems, however, call for a mix of implicit and explicit techniques. These problems occur when the high stiffness is due to only a part of the model. This typically happens when a small number of elements with high diffusivity or short conduction lengths are used. Recently, several promising techniques have been developed which combine the attributes of explicit and implicit integration techniques. These techniques are referred to as partitioning techniques and are still in the research stage in contrast to the more mature status of the purely explicit and implicit integration techniques. A survey of partitioning methods may be found in reference 28. This section presents examples of the use of such methods for transient thermal analysis.

The Hughes-Liu Mixed Explicit-Implicit Technique

One class of partitioning methods is based on dividing the model into explicit and implicit parts. The Hughes-Liu mixed implicit-explicit technique, which was originally developed for problems with fluid structure interaction (refs. 17 and 18), is an example of such a partitioning method. The basic idea is to use implicit integration for the portion of the model which is responsible for the stiffness of the problem and explicit integration for the rest of the model. This idea was adapted by Malkus, Reichmann, and Haftka (ref. 19) to transient heat transfer in a structure which is composed of a good insulator and a good conductor. The structure is divided into an explicit group of elements and an implicit group of elements. Equation (1) is then rewritten as

$$2C\,\frac{T_{n+1} - T_n}{h_n} + K^I(T_n + T_{n+1}) + 2K^E T_n - Q(T_n) - Q(T_{n+1}) = 0 \qquad (9)$$

where K^E is the partition of the conductivity matrix corresponding to the elements in the explicit group, and K^I is the partition for the elements in the implicit group. When all the elements are explicit, the method reduces to the explicit Euler method; when all the elements are implicit, the method reduces to the implicit Crank-Nicholson method. The method was applied to the configuration in figure 16 which is a coarse model of one-half the configuration in figure 3. The insulation finite elements are in the explicit group; the metal finite elements are in the implicit group. The diffusion ratio between the insulation and the metal was kept constant at 50, whereas the absolute values of the diffusivity were changed to control the stiffness of the problem. Table 5 contains two sets of results comparing the calculation times for the fully explicit (Euler), fully implicit (Crank-Nicholson), and Hughes-Liu techniques for two values of the diffusivities. For the lower value of the diffusivity, the problem is not stiff and the explicit method performs better than the implicit method. In this case, the Hughes-Liu method is comparable in performance to the explicit method. For the higher value of the diffusivity (higher stiffness), the implicit method is faster than the explicit method because of the stiffness of the problem. In this case, the Hughes-Liu technique is significantly better than either the explicit or the implicit method. This simple example indicates the potential of the Hughes-Liu technique for improving the efficiency of transient thermal analysis for more complicated insulated-structure problems.

Operator-Splitting Algorithms for Linear Equations

The Hughes-Liu technique represents partitioning at the level of integration of the differential equations. Other partitioning methods may be appropriate later in the solution process. An important class of these methods are used in the solution of the linear algebraic equations generated by Newton's method utilized in implicit solution techniques (eqs. (7) and (8)). For notational simplicity, the equations generated by Newton's method are written as

$$Ax = b \tag{10}$$

Operator-splitting methods are based on separating the matrix A into two parts M and N such that

$$A = M - N \tag{11}$$

Equations (10) and (11) are combined and the resulting equation is solved iteratively. A simple fixed-point iteration is used

$$x^{m+1} = M^{-1}(b + Nx^m) \tag{12}$$

This iteration may be modified to include an overrelaxation parameter ω and is written as follows:

$$x^{m+1} = \omega M^{-1}(b + Nx^m) + (1 - \omega)x^m \tag{13}$$

The choice of M and N is based on the following general considerations. First, the matrix M should be significantly easier to invert than the matrix A. Second, it should be chosen for fast convergence of the iteration in equation (13). The choice of M may also be based on matrix topology considerations - for example, the sparsity of the matrices A and M - or it may be based on the properties of the mathematical model that led to matrix A. Consider the latter choice first.

Operator splitting based on model characteristics.- If the problem is composed of a good conductor and a good insulator, the splitting (which parallels the Hughes-Liu technique) is to include in M the contribution of the good conductor and the diagonal term from the good insulator. This choice was applied to the analysis of a simple metal insulation system (shown in fig. 17) by David S. Malkus, Elwood T. Olsen, Peter I. Reichmann, and Raphael T. Haftka under NASA Grant NSG-1266 at Illinois Institute of Technology. This model depicts an insulated slab heated by internal sources and cooled at the outer insulation surface by radiation to free space. The Crank-Nicholson algorithm with the modified Newton's method was used to generate the equations to be solved. Computation times with and without operator splitting were compared for several grids. The results are given in table 6. Though the splitting was effective (from the standpoint that the solution of eq. (13) required only a single iteration), the results in table 6 are somewhat disappointing. The results indicate this type of operator splitting is effective only if frequent factoring of the Jacobian is needed.

Operator splitting based on matrix structure.- Several choices for the matrices M and N based on the matrix topology are available. Two obvious choices that result in an easily invertible M matrix are the diagonal of matrix A and the lower triangular part of A. These choices lead to the well-known Jacobi and Gauss-Seidel iterative methods, respectively. The Gauss-Seidel iteration with over-relaxation is commonly known as successive overrelaxation (SOR). Although matrices based on the above are easily inverted, they usually result in slow convergence of the iteration process. When the matrix A is very sparse and has a large bandwidth (as when it is generated by a three-dimensional finite-element model), a choice of M which is based on a partial elimination or incomplete Cholesky decomposition that retains the sparsity of A has been suggested. In this case,

$$M = LL^T \tag{14}$$

where L is a lower triangular matrix which has the same sparsity pattern as A. This incomplete Cholesky decomposition has been combined with the conjugate gradient method by Meijerink and Van der Vorst (ref. 20) to produce the incomplete Cholesky conjugate gradient (ICCG) algorithm. The conjugate gradient method forms the basis for other iterative algorithms, such as preconditioned conjugate gradient methods (e.g., ref. 29). The algorithm has been applied by Haftka and Kadivar (ref. 30) to the insulated cylinder problem. For this problem four methods were compared: (1) Gaussian elimination (a direct solution technique); (2) SOR; (3) incomplete Cholesky decomposition with fixed-point iteration (eq. (12)); and (4) the ICCG algorithm. Results are shown in figure 18 for cylinder models having 400, 720, and 1100 grid points. These results demonstrate the advantages of iterative methods over elimination, especially for poorly banded problems. Also, the ICCG algorithm is consistently superior, for the problem studied, to the two other iterative procedures and is nearly independent of the matrix bandwidth but depends on the degree of sparsity.

CONCLUDING REMARKS

This paper discussed an effort to obtain increased efficiency in calculating transient temperature fields in complex aerospace vehicle structures. Explicit solution techniques which require minimal computation per time step and implicit techniques which permit larger time steps because of better stability were reviewed. A promising set of implicit solution algorithms having variable time steps and order, known as GEARIB, was described. Test problems for evaluating the algorithms were defined and finite-element models of each one were described. The problems included a coarse model of the Space Shuttle Orbiter wing, an insulated frame test article, a metallic panel for a thermal protection system, and detailed models of single-bay and three-bay sections of the Shuttle wing. Calculations were carried out using the SPAR finite-element program. Results generally indicated that implicit algorithms, particularly the GEARIB techniques, are more efficient than explicit algorithms for solution of transient structural heat-transfer problems when the governing equations are stiff. Stiff equations were encountered in most of the test problems and are frequently encountered in thermal analysis of insulated thin metal structures.

Studies were made of the effect on algorithm performance of different models of an insulated cylinder test problem. These studies revealed that the stiffness of the problem is highly sensitive to modeling details and that careful modeling can reduce the stiffness of the resulting equations to the extent that explicit methods are quite effective.

Evaluations of two partitioning techniques were also performed. First, a mixed implicit-explicit technique adapted to thermal analysis was demonstrated. In this method, the model is separated into stiff and nonstiff portions with the explicit algorithm applied to the nonstiff part and the implicit algorithm applied to the stiff part. This method was comparable in performance to the explicit method for a nonstiff problem and faster than either the explicit or implicit techniques for stiff problems. Second, two operator-splitting techniques for speeding up the solution of the algebraic equations associated with implicit algorithms were described and demonstrated. Both are based on separating the coefficient matrices into two parts and solving the resulting equations by iteration. The first technique bases the separation on stiff and nonstiff elements of the structure, and the second bases the separation on the sparsity structure of the matrix. The most effective of the techniques tried was a separation based on matrix sparsity (using an incomplete Cholesky decomposition) with conjugate gradient iteration. This technique was especially noteworthy in that its performance appeared to be insensitive to the band structure of the matrix.

Langley Research Center
National Aeronautics and Space Administration
Hampton, VA 23665
July 1, 1982

REFERENCES

1. Willoughby, Ralph A., ed.: Stiff Differential Systems. Plenum Press, c.1974.

2. Wilson, Edward L.; and Nickell, Robert E.: Application of the Finite Element Method to Heat Conduction Analysis. Nucl. Eng. & Des., vol. 4, no. 3, Oct. 1966, pp. 276-286.

3. Wilson, E. L.; Bathe, K. J.; and Peterson, F. E.: Finite Element Analysis of Linear and Nonlinear Heat Transfer. Nucl. Eng. & Des., vol. 29, 1974, pp. 110-124.

4. Hughes, Thomas J. R.: Unconditionally Stable Algorithms for Nonlinear Heat Conduction. Comput. Methods Appl. Mech. & Eng., vol. 10, no. 2, Feb. 1977, pp. 135-139.

5. Bathe, Klaus-Jürgen; and Khoshgoftaar, Mohammad R.: Finite Element Formulation and Solution of Nonlinear Heat Transfer. Nucl. Eng. & Des., vol. 51, 1979, pp. 389-401.

6. Hogge, M. A.: Integration Operators for First Order Linear Matrix Differential Equations. Comput. Methods Appl. Mech. & Eng., vol. 11, no. 3, June-July 1977, pp. 281-294.

7. Wood, W. L.; and Lewis, R. W.: A Comparison of Time Marching Schemes for the Transient Heat Conduction Equation. Int. J. Numer. Methods Eng., vol. 9, no. 3, 1975, pp. 679-289.

8. Marlowe, M. B.; Moore, R. A.; and Whetstone, W. D.: SPAR Thermal Analysis Processors Reference Manual, System Level 16. NASA CR-159162, 1979.

9. Trent, Donald S.; and Welty, James R.: A Summary of Numerical Methods for Solving Transient Heat Conduction Problems. Bull. No. 49, Eng. Exp. Stn., Oregon State Univ., Oct. 1974.

10. Krinke, Dennis C.; and Huston, Ronald L.: An Analysis of Algorithms for Solving Differntial Equations. Comput. & Struct., vol. 11, no. 1-2, Feb. 1980, pp. 69-74.

11. Argyris, J. H.; St. Doltsinis, J.; Knudson, W. C.; Vaz, L. E.; and William, K. J.: Numerical Solution of Transient Nonlinear Problems. Comput. Methods Appl. Mech. & Eng., vol. 17/18, pt. II, Feb. 1979, pp. 341-409.

12. Shampine, L. F.; and Gear, C. W.: A User's View of Solving Stiff Ordinary Differential Equations. SIAM Rev., vol. 21, no. 1, Jan. 1979, pp. 1-17.

13. Hindmarsh, A. C.: A Collection of Software for Ordinary Differential Equations. American Nuclear Society Proceedings of the Topical Meeting on Computational Methods in Nuclear Engineering - Volume 3, Apr. 1979, pp. 8-1 - 8-15.

14. Gear, C. William: Numerical Initial Value Problems in Ordinary Differential Equations. Prentice-Hall, Inc., c.1971.

15. Byrne, G. D.; and Hindmarsh, A. C.: A Polyalgorithm for the Numerical Solution of Ordinary Differential Equations. ACM Trans. Math. Software, vol. 1, no. 1, Mar. 1975, pp. 71-96.

16. Adelman, H. M.; Haftka, R. T.; and Robinson, J. C.: Some Aspects of Algorithm Performance and Modeling in Transient Thermal Analysis of Structures. 81-WA/HT-4, American Soc. Mech. Eng., Nov. 1981.

17. Hughes, T. J. R.; and Liu, W. K.: Implicit-Explicit Finite Elements in Transient Analysis: Stability Theory. Trans. ASME, J. Appl. Mech., vol. 45, no. 2, June 1978, pp. 371-374.

18. Hughes, T. J. R.; and Liu, W. K.: Implicit-Explicit Finite Elements in Transient Analysis: Implementation and Numerical Examples. Trans. ASME, J. Appl. Mech., vol. 45, no. 2, June 1978, pp. 375-378.

19. Malkus, David S.; Reichmann, Peter I.; and Haftka, Raphael T.: Application of the Hughes-Liu Algorithm to the Two-Dimensional Heat Equation. NASA CR-3599, 1982.

20. Meijerink, J. A.; and Van der Vorst, H. A.: An Iterative Solution Method for Linear Systems of Which the Coefficient Matrix is a Symmetric M-Matrix. Math. Comput., vol. 31, no. 137, Jan. 1977, pp. 148-162.

21. Adelman, Howard M.; and Haftka, Raphael T.: On the Performance of Explicit and Implicit Algorithms for Transient Thermal Analysis of Structures. NASA TM-81880, 1980.

22. Gallegos, J. J.: Thermal Math Model Analysis of FRSI Test Article Subjected to Cold Soak and Entry Environments. A Collection of Technical Papers - AIAA/IES/ASTM 10th Space Simulation Conference, Oct. 1978, pp. 131-136. (Available as AIAA Paper 78-1627.)

23. Jackson, L. Robert; and Dixon, Sidney C.: A Design Assessment of Multiwall, Metallic Stand-Off, and RSI Reusable Thermal Protection Systems Including Space Shuttle Application. NASA TM-81780, 1980.

24. Goble, R. G.; and Jensen, C. L.: Thermal Radiation Analysis System TRASYS II - User's Manual. NASA CR-159273-1, 1980.

25. Ko, William L.; Quinn, Robert D.; Gong, Leslie; Schuster, Lawrence S.; and Gonzales, David: Reentry Heat Transfer Analysis of the Space Shuttle Orbiter. Computational Aspects of Heat Transfer in Structures, NASA CP-2216, 1982, pp. 295-325.

26. Martin Interactive Thermal Analyzer System - Version 1.0. User's Manual. MDS-SPLPD-71-FD238 (REV 3), Martin Marietta Corp., Mar. 1972.

27. Sperry Support Services: Creation of Lumped Parameter Thermal Model by the Use of Finite Elements. NASA CR-158944, 1978.

28. Park, K. C.: Partitioned Transient Analysis Procedures for Coupled-Field Problems: Stability Analysis. Trans. ASME, J. Appl. Mech., vol. 47, no. 2, June 1980, pp. 370-376.

29. Axelsson, O.; and Munksgaard, N.: A Class of Preconditioned Conjugate Gradient Methods for the Solution of a Mixed Finite Element Discretization of the Biharmonic Operator. Int. J. Numer. Methods Eng., vol. 14, no. 7, 1979, pp. 1001-1019.

30. Haftka, Raphael T.; and Kadivar, M. Hassan: Algorithmic Aspects of Transient Heat Transfer Problems in Structures. Computational Aspects of Heat Transfer in Structures, NASA CP-2216, 1982, pp. 99-114.

TABLE 1.- PERFORMANCE OF ALGORITHMS FOR TRANSIENT THERMAL ANALYSIS OF VARIOUS MODELS

[Solution time is CPU time]

Explicit algorithm		Implicit algorithm			
Euler		Crank-Nicholson		GEARIB	
Time step, sec	Solution time, sec	Time step, sec	Solution time, sec	Time step, sec	Solution time, sec
(a) Space Shuttle Orbiter wing (4500-sec temperature history)					
10	2 288	10	11 730	1 to 528	570
(b) Shuttle frame (2000-sec temperature history)					
0.16	1 723	1 10 25 50	475 249 106 65	50 to 170	54
(c) Multiwall thermal protection system (3200-sec temperature history)					
0.007	[a]98 400	1 5	[b]28 400 6 352	1.0 to 113	2754
(d) Three-bay section of Shuttle wing (3500-sec temperature history)					
2.6	10 560	5	16 800	0.1 to 229	1950
(e) Single-bay section of Shuttle wing (3500-sec temperature history)					
0.1	3 205	1	1 145	0.1 to 225	245

[a]Extrapolated value based on 12 296 seconds for 400 seconds of temperature history.

[b]Extrapolated value based on 8879 seconds for 1000 seconds of temperature history.

TABLE 2.- EFFECT OF TIME STEP ON ACCURACY OF IMPLICIT ALGORITHMS FOR SHUTTLE FRAME

Time step, sec	Temperature of node 309[a] at 1200 sec, °F	Temperature of node 49[a] at 1200 sec, °F
1.0	335.7	398.6
10.0	335.6	398.5
25.0	331.6	396.0
50.0	328.3	394.7
[b].16	335.7	398.6
[c]50 to 170	337.5	400.3

[a]See figure 3(b).
[b]Explicit algorithm.
[c]GEARIB.

TABLE 3.- EFFECT OF MODELING ON SOLUTION TIME FOR INSULATED CYLINDER PROBLEM

[Solution time is CPU time]

Model	Explicit algorithm		Implicit algorithm			
	Euler		Crank-Nicholson and backward-difference		GEARIB	
	Time step, sec	Solution time, sec	Time step, sec	Solution time, sec	Time step, sec	Solution time, sec
SPAR model I	0.06	10 107	10	1880	1.0 to 83	1779
SPAR model II	2.4 to 10	1 518	10	1920	5 to 106	1707
SPAR model III	3.3 to 10	279	10	536	2 to 133	266
MITAS lumped-parameter model	10	226	10	320		

TABLE 4.- EFFECT OF MATRIX SCALING ON SOLUTION TIME FOR INSULATED CYLINDER PROBLEM

[Solution time is CPU time]

Model	Explicit algorithm		Implicit algorithm			
	Euler		Crank-Nicholson		GEARIB	
	Time step, sec	Solution time, sec	Time step, sec	Solution time, sec	Time step, sec	Solution time, sec
SPAR model I						
With scaling	0.06	8 000	10	735	1 to 83	520
Without scaling	0.06	10 107	10	1880	1 to 83	1779
SPAR model II						
With scaling	2.4 to 10	392	10	782	5 to 106	505
Without scaling	2.4 to 10	1 518	10	1920	5 to 106	1707
SPAR model III						
With scaling	3.3 to 10	247	10	504	2 to 133	231
Without scaling	3.3 to 10	279	10	536	2 to 133	266

TABLE 5.- EVALUATION OF HUGHES-LIU IMPLICIT-ALGORITHM FOR TRANSIENT THERMAL ANALYSIS OF INSULATED STRUCTURE

[Solution time is CPU time on Prime 400 computer]

Degree of stiffness	k, Btu/in-sec-°F, for -		ρc_p, Btu/in^3-°F, for -		Method	Solution time, sec
	Metal	Insulation	Metal	Insulation		
Low	0.002	1.57×10^{-6}	0.02	8.11×10^{-4}	Implicit (Crank-Nicholson) Explicit (Euler) Implicit-explicit (Hughes-Liu)	129 83 77
High	0.02	1.57×10^{-5}	0.02	8.11×10^{-4}	Implicit (Crank-Nicholson) Explicit (Euler) Implicit-explicit (Hughes-Liu)	245 635 158

TABLE 6.- EFFECT OF OPERATOR SPLITTING ON SOLUTION TIME FOR INSULATED SLAB

[Solution time is CPU time on Prime 400 computer]

Mesh	Number of time steps	Number of factorings	Solution time, sec, for -	
			Modified Newton's method without splitting	Modified Newton's operator method with splitting
7 × 7 × 1	91	20	119	149
7 × 7 × 1	52	26	95	99
7 × 7 × 1	51	51	137	117
7 × 11 × 1	91	20	237	340
7 × 11 × 1	51	51	234	223
7 × 7 × 2	91	20	1205	1129
7 × 7 × 2	52	26	1164	752
7 × 7 × 2	51	51	1911	928

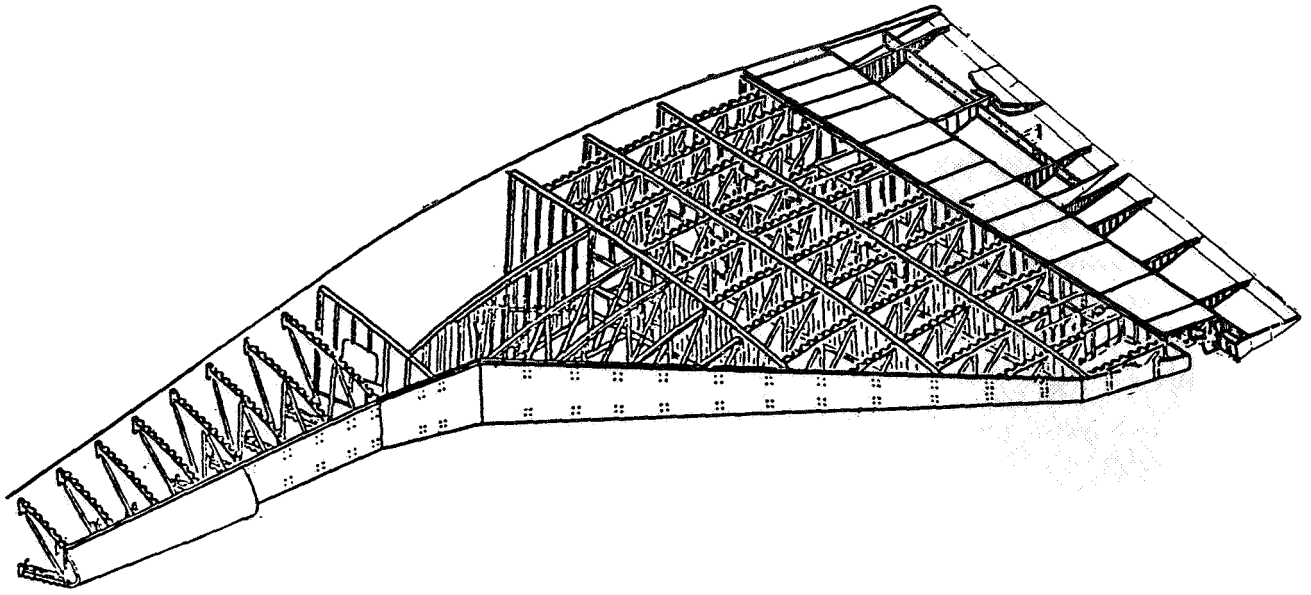

(a) Configuration.

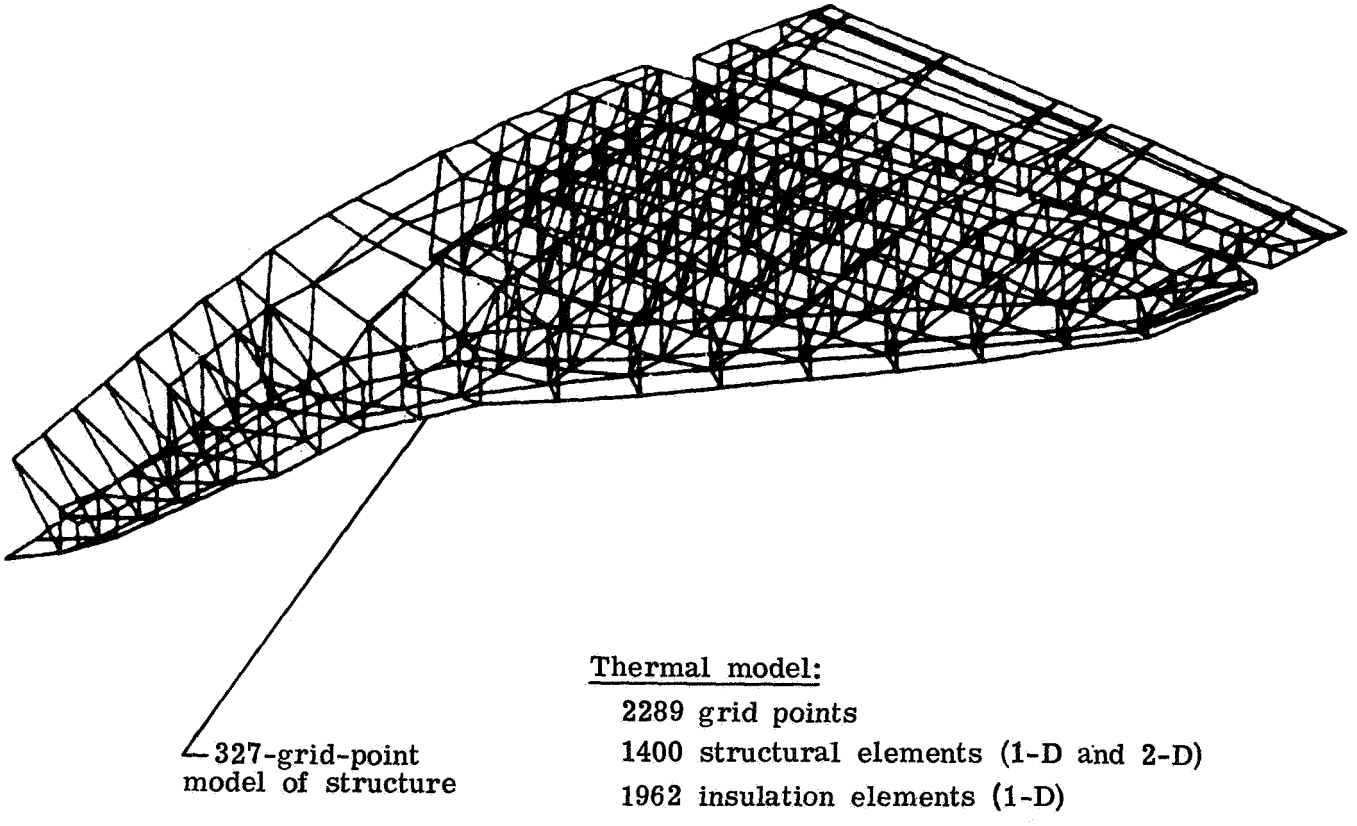

(b) Finite-element model.

Figure 1.- Space Shuttle Orbiter wing.

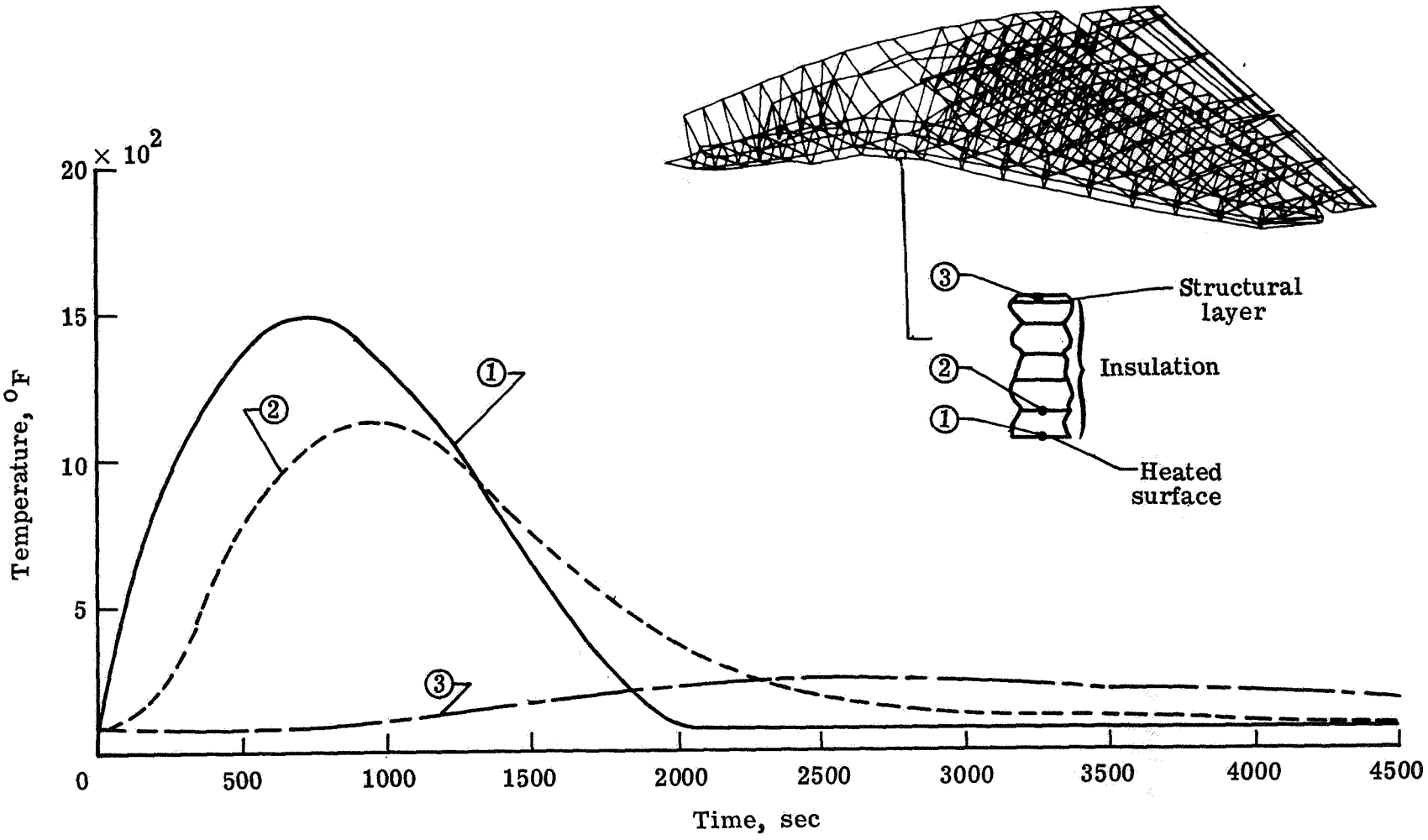

Figure 2.- Transient temperatures in Shuttle Orbiter wing.

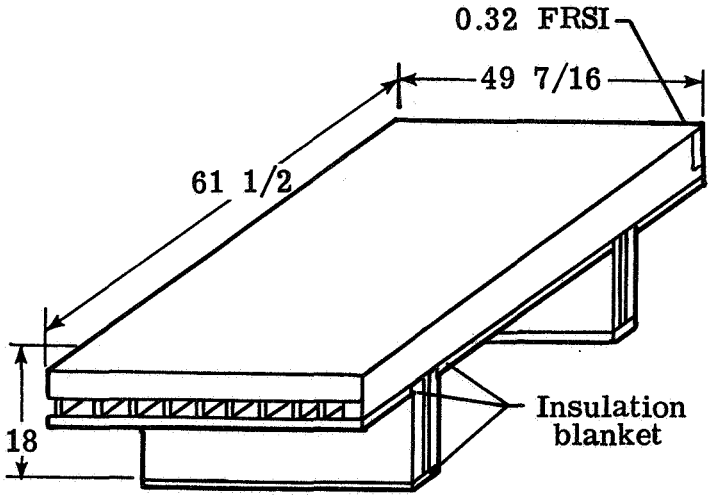

(a) Configuration. All dimensions are in inches.

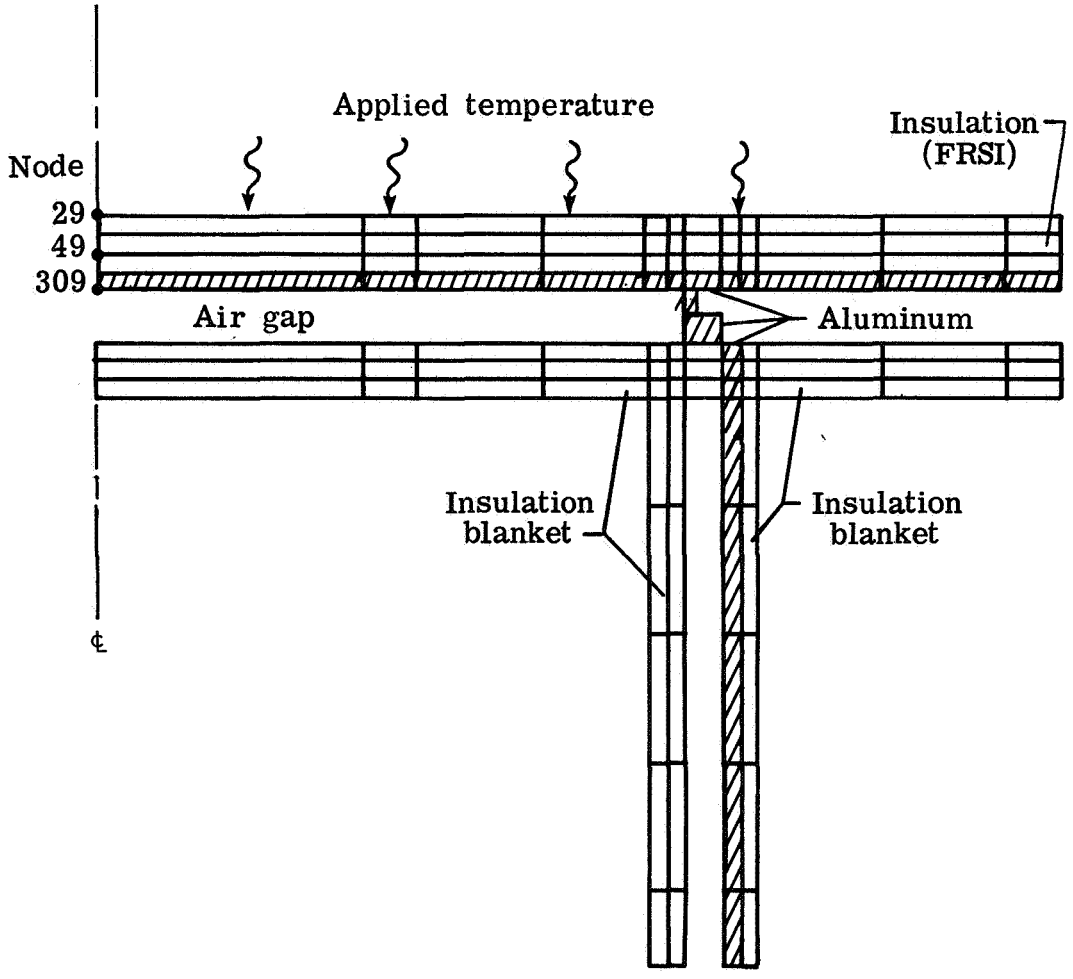

(b) Finite-element model.

Figure 3.- Insulated frame test article. (From ref. 22.)

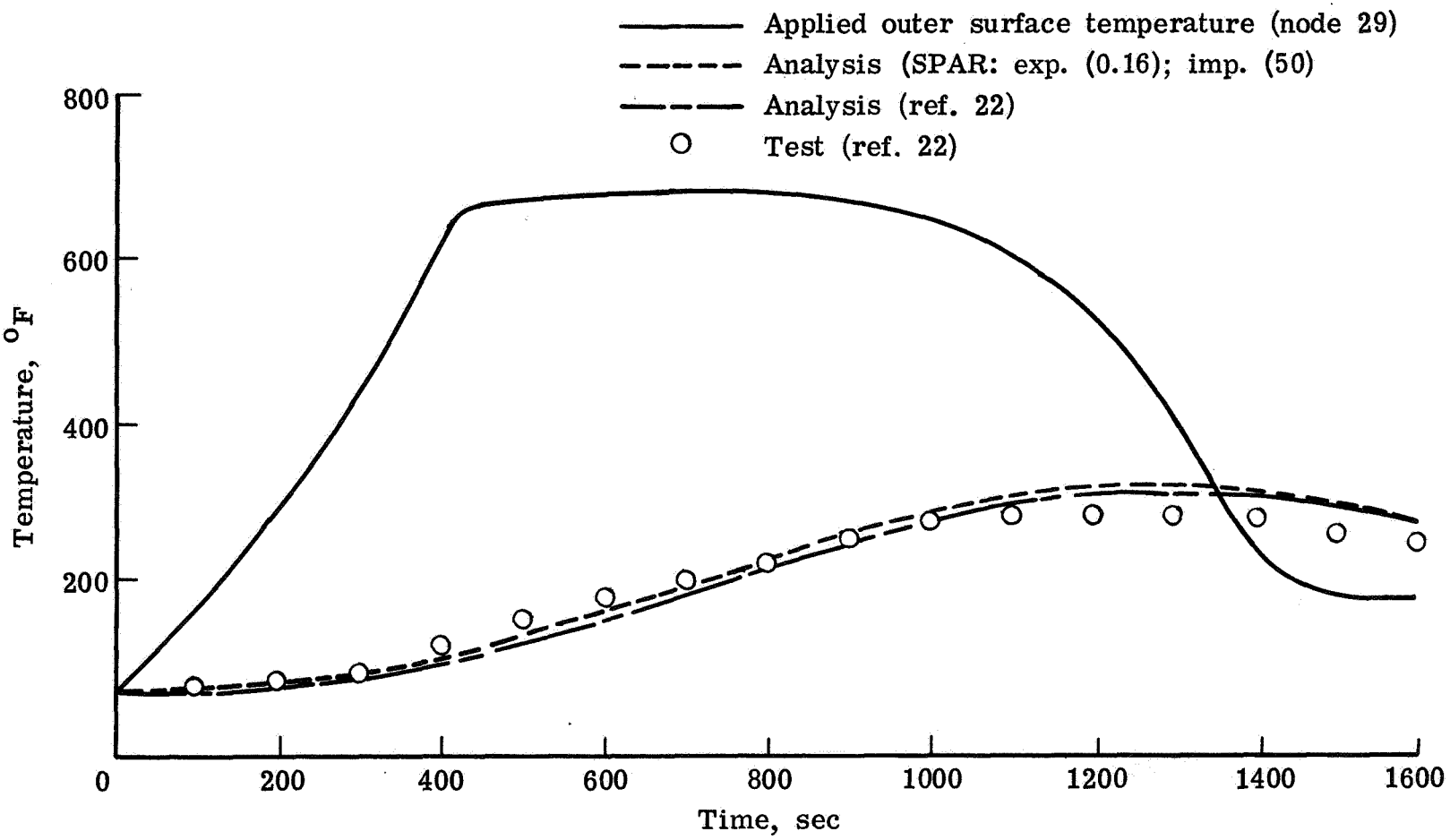

Figure 4.- Temperature history in outer structural surface of Shuttle frame (node 309). Numbers in parentheses are values of DT in seconds.

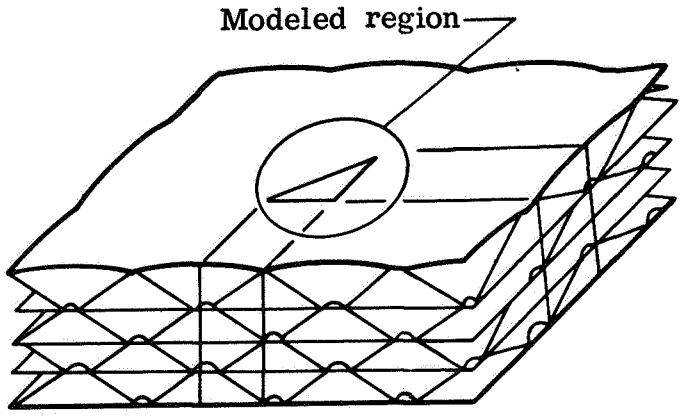

(a) Overall construction.

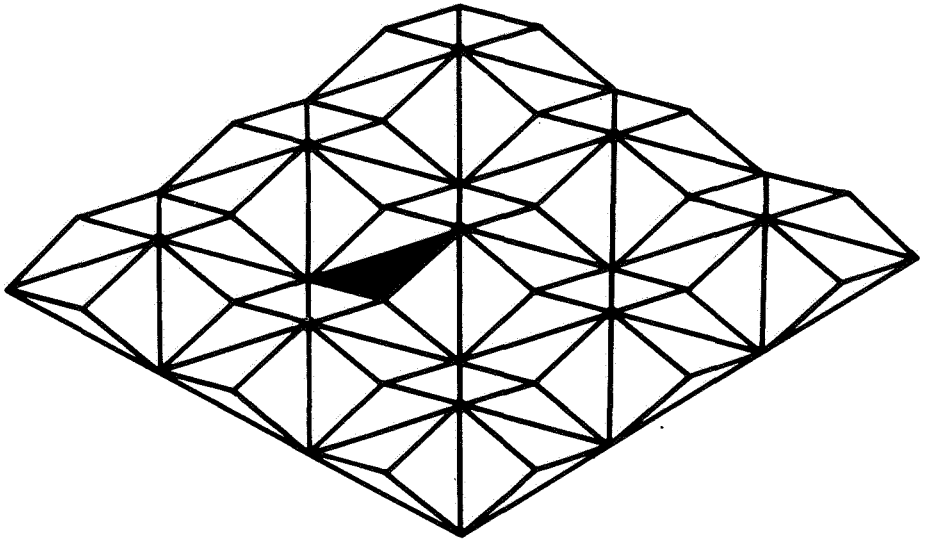

(b) Representation of dimpled layer.

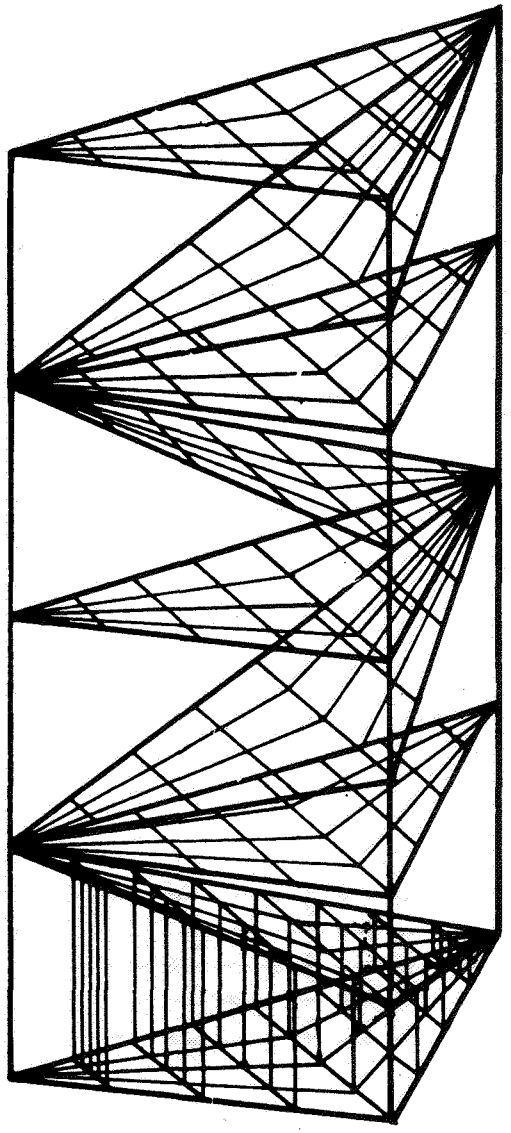

(c) Finite-element model. Internal vertical lines are omitted for clarity except in lowest level.

Figure 5.- Multiwall thermal protection system panel.

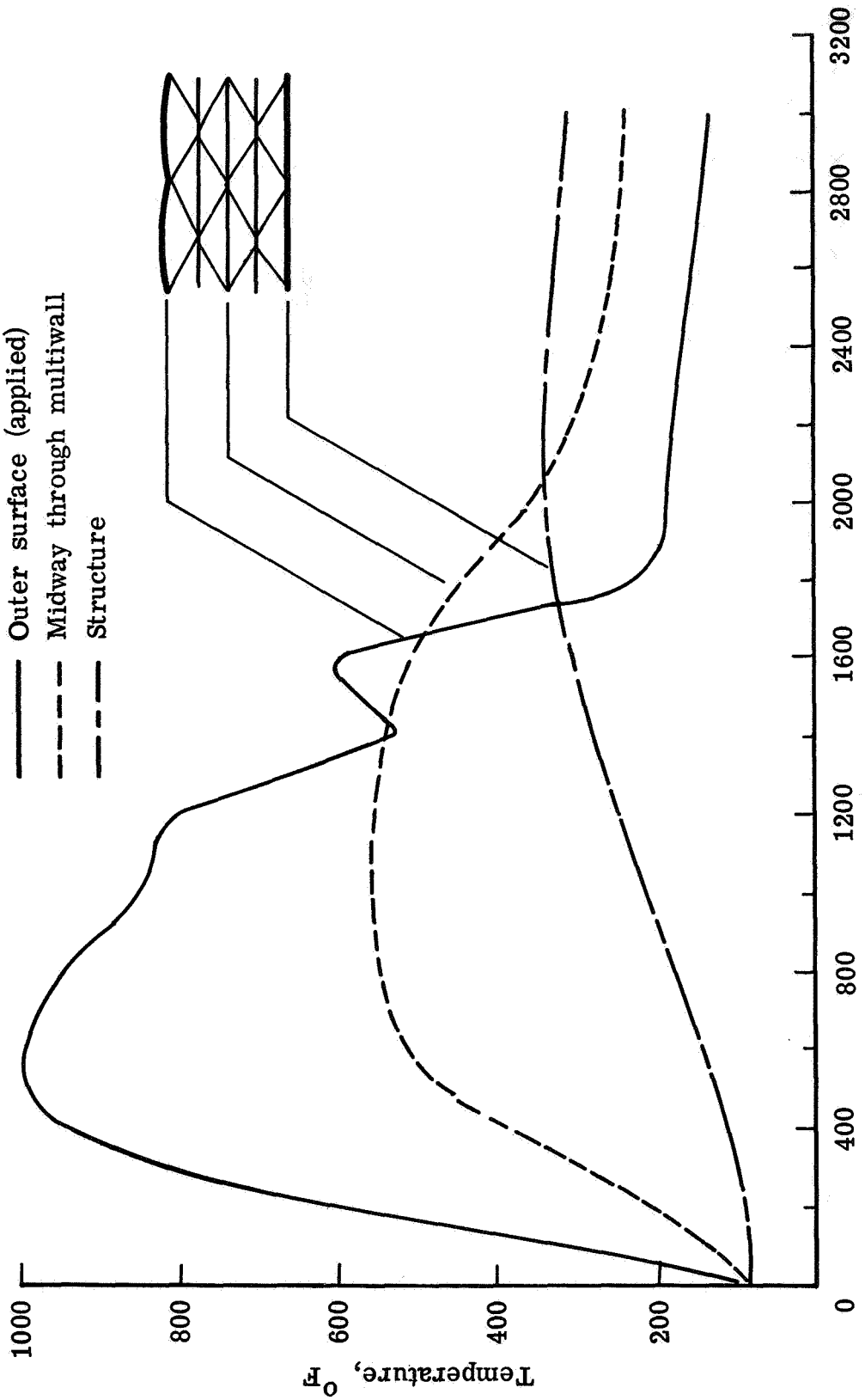

Figure 6.- Transient temperatures in titanium multiwall TPS panel.

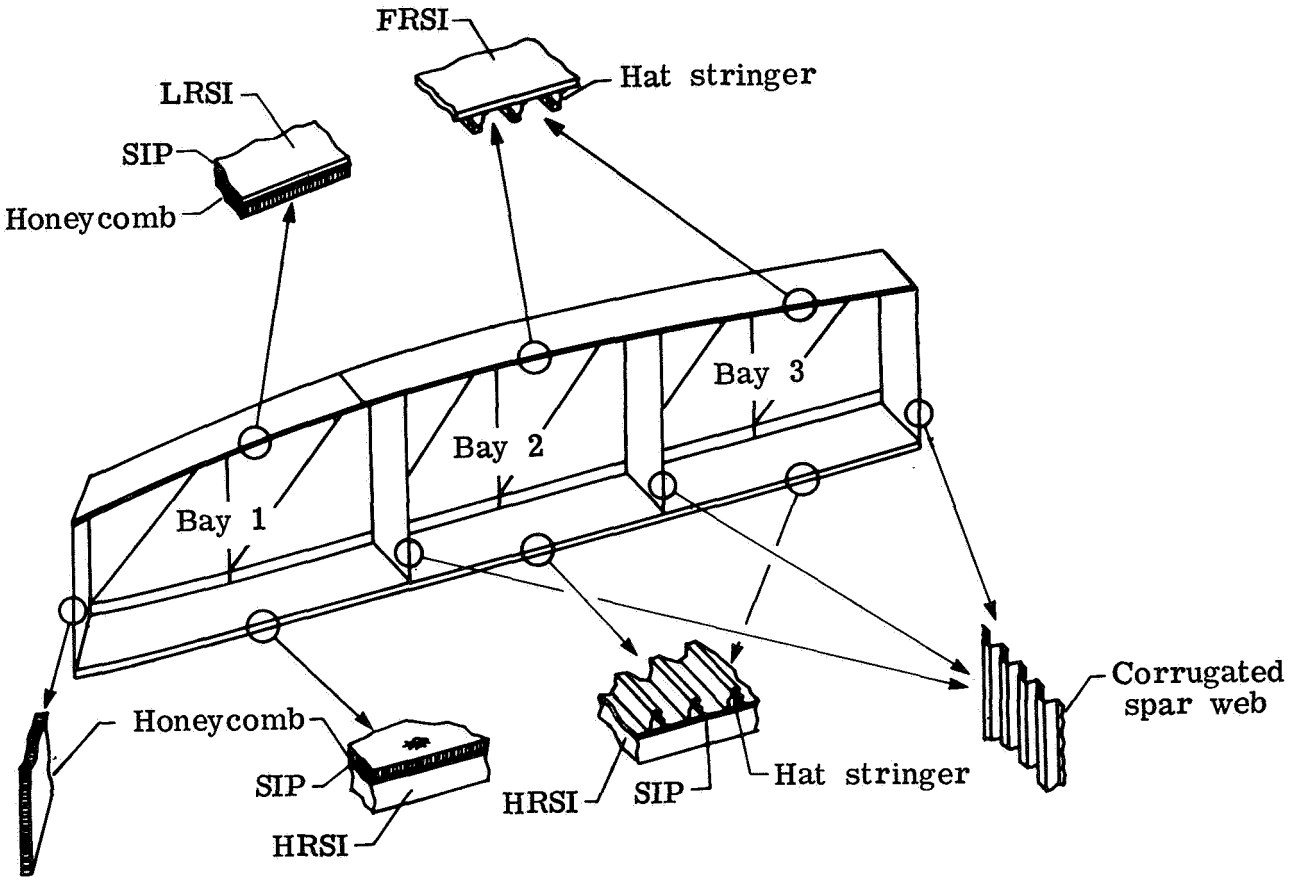

Figure 7.- Some construction details of Shuttle wing at wing stations 240 and 328. (From ref. 25.)

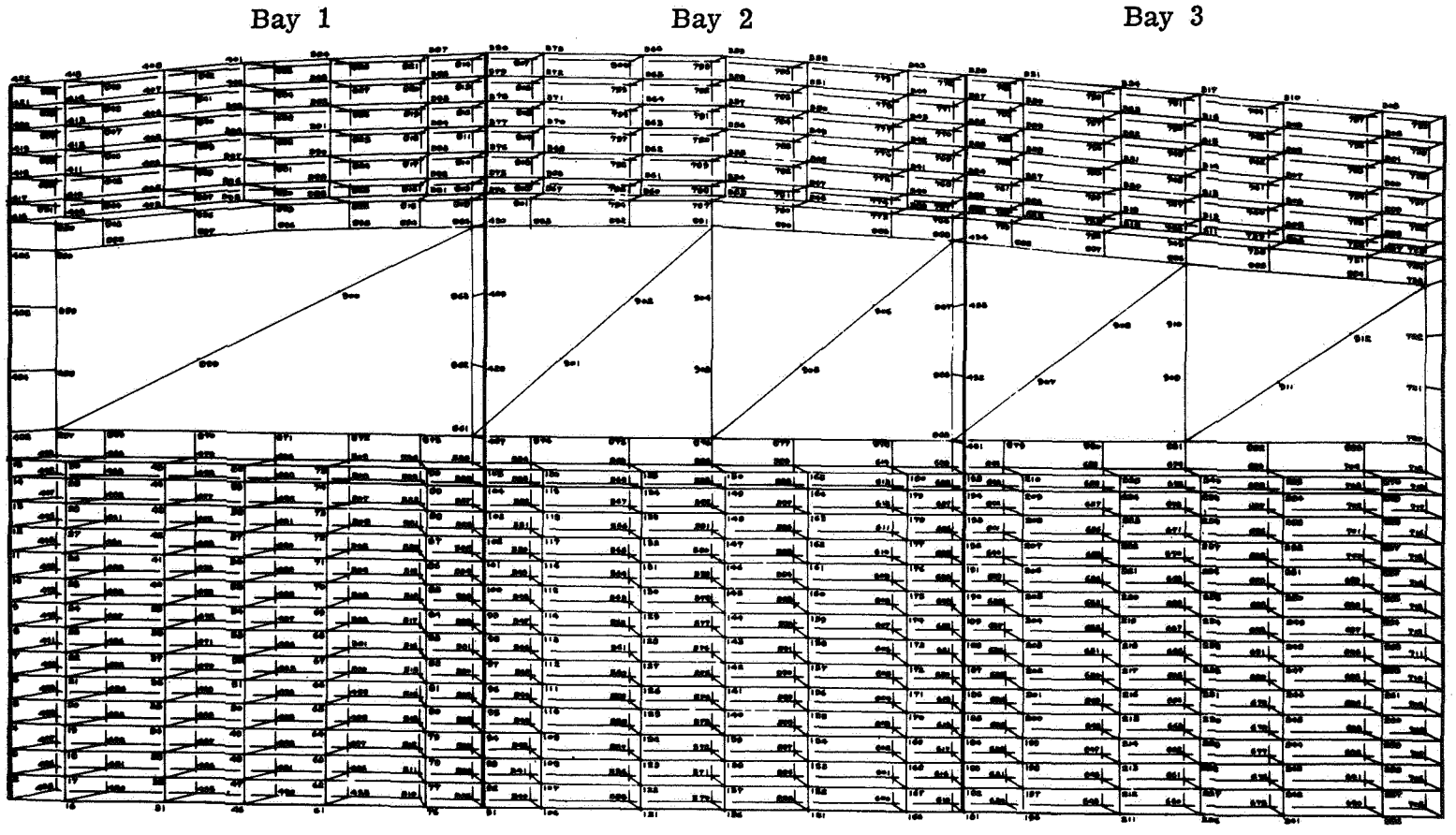

Figure 8.- Finite-element model of three-bay section of Shuttle wing (wing station 328). (From ref. 25.)

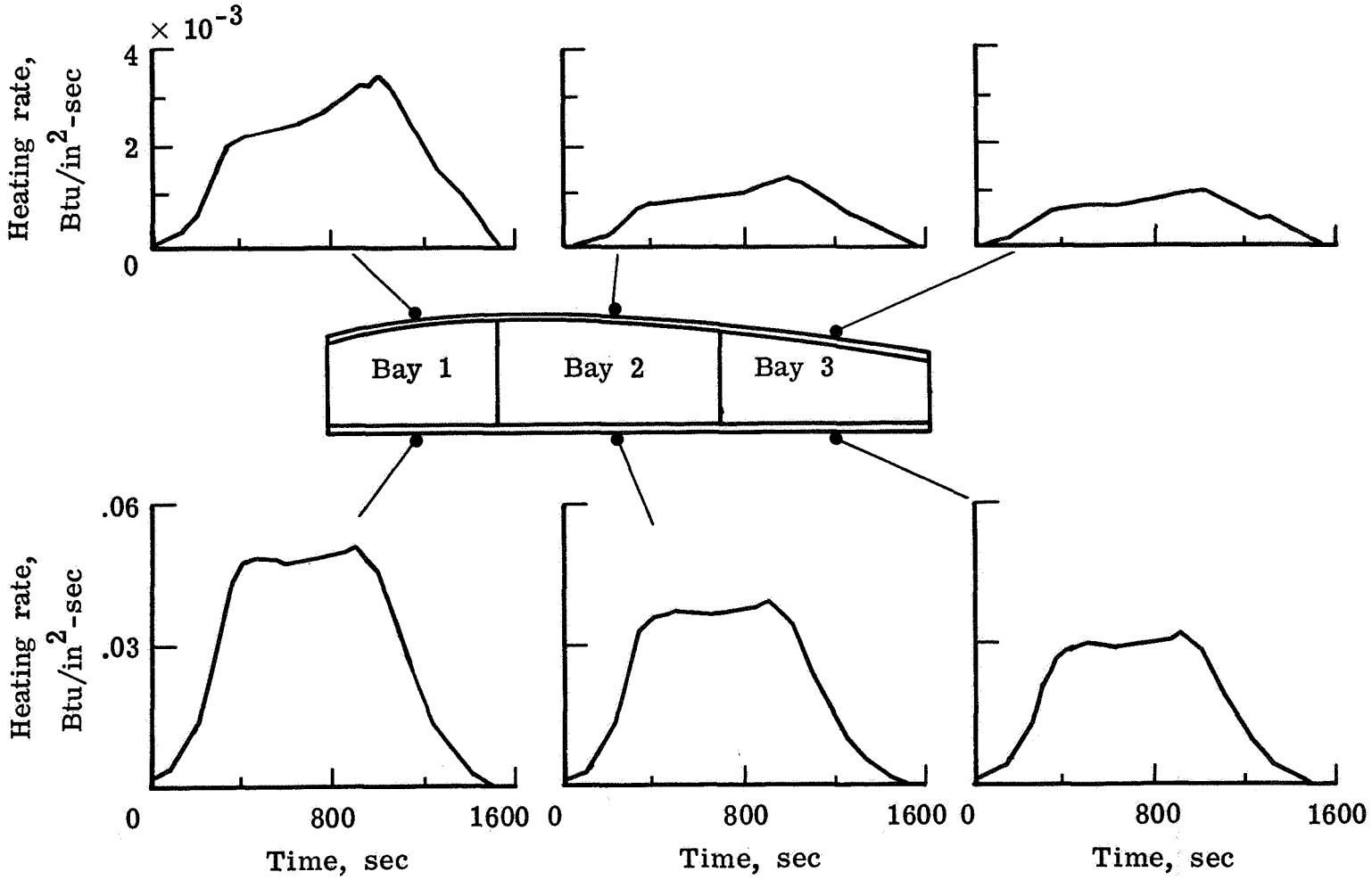

Figure 9.- Heating rates on model of three-bay section of Shuttle wing. (From ref. 25.)

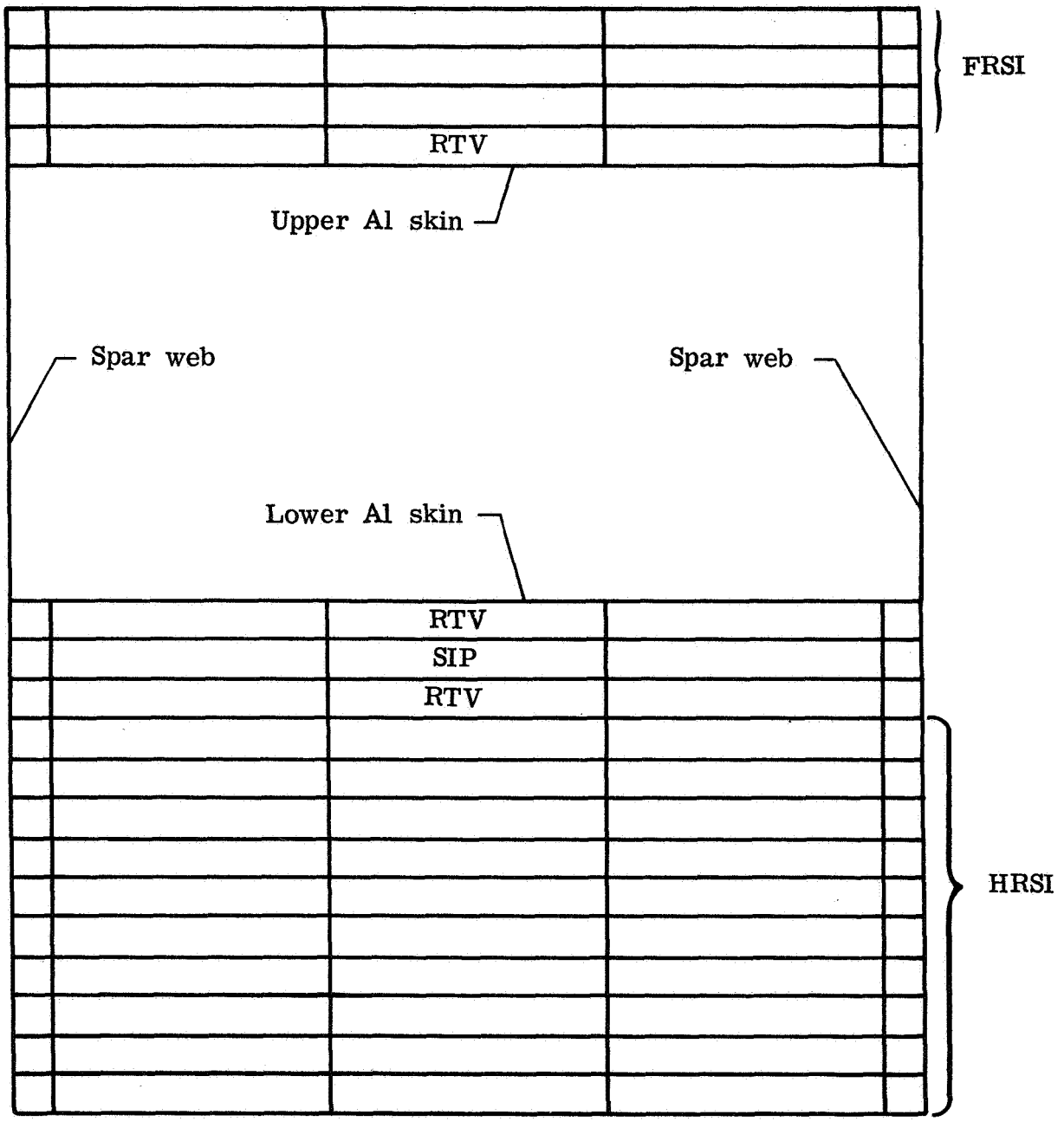

Figure 10.- Finite-element model of Shuttle wing bay at wing station 240.

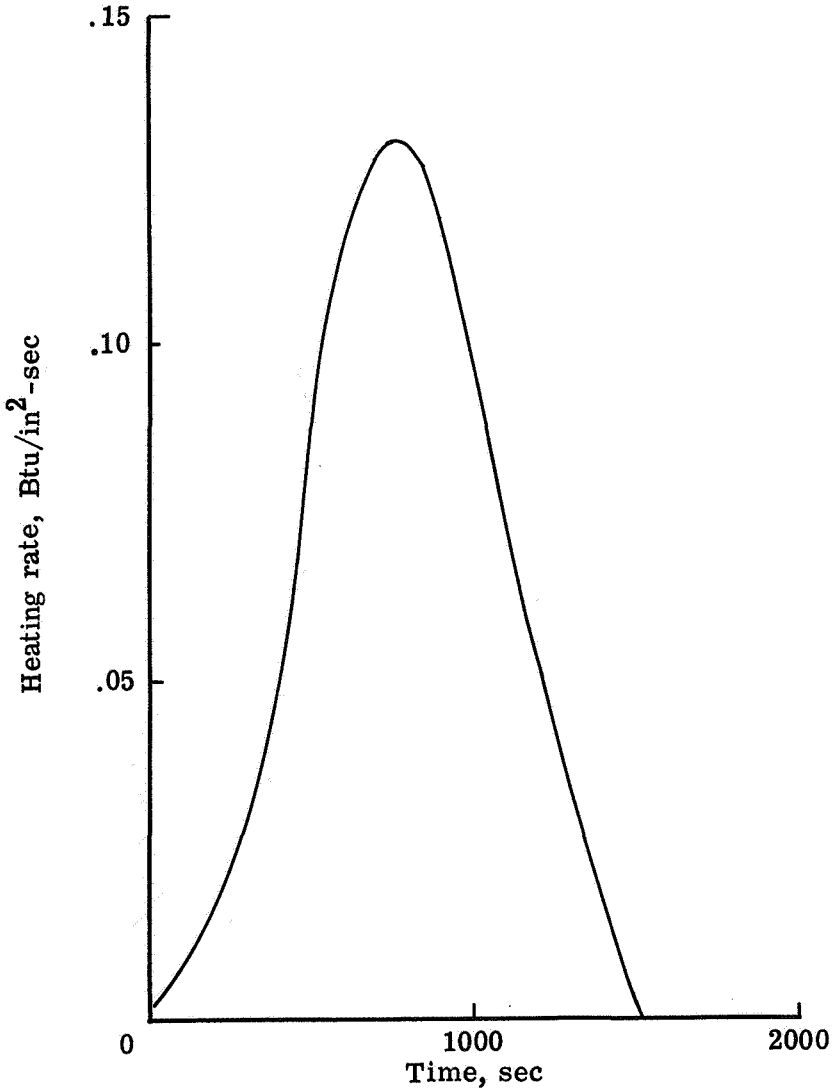

(a) Lower surface.

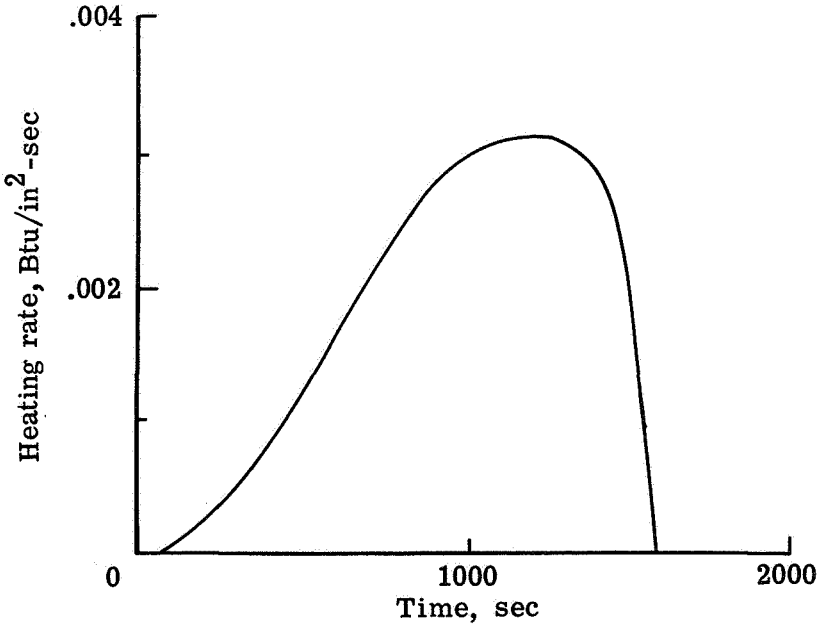

(b) Upper surface.

Figure 11.- Heating rates on single bay of Shuttle wing.

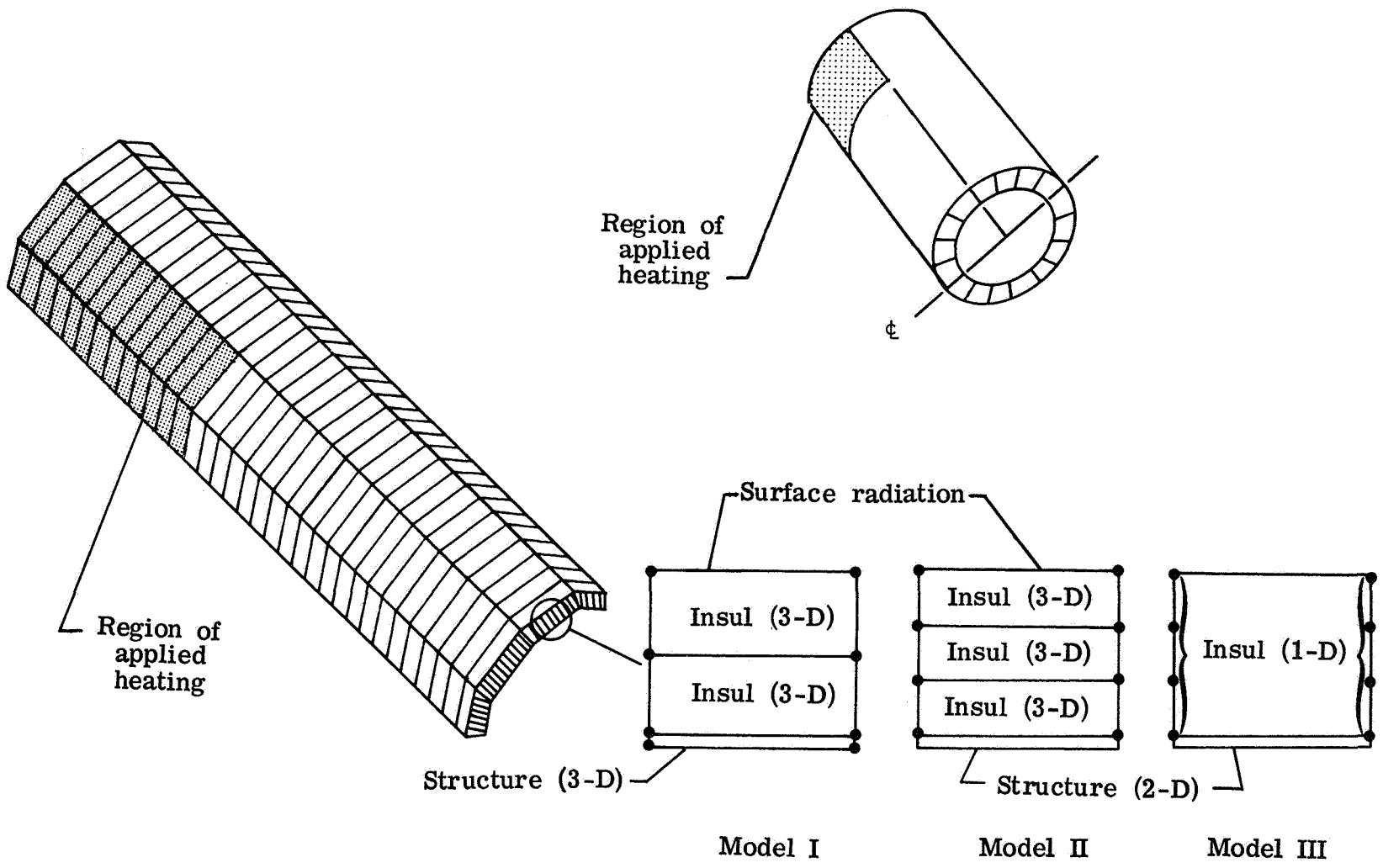

Figure 12.- Finite-element models of insulated cylinder.

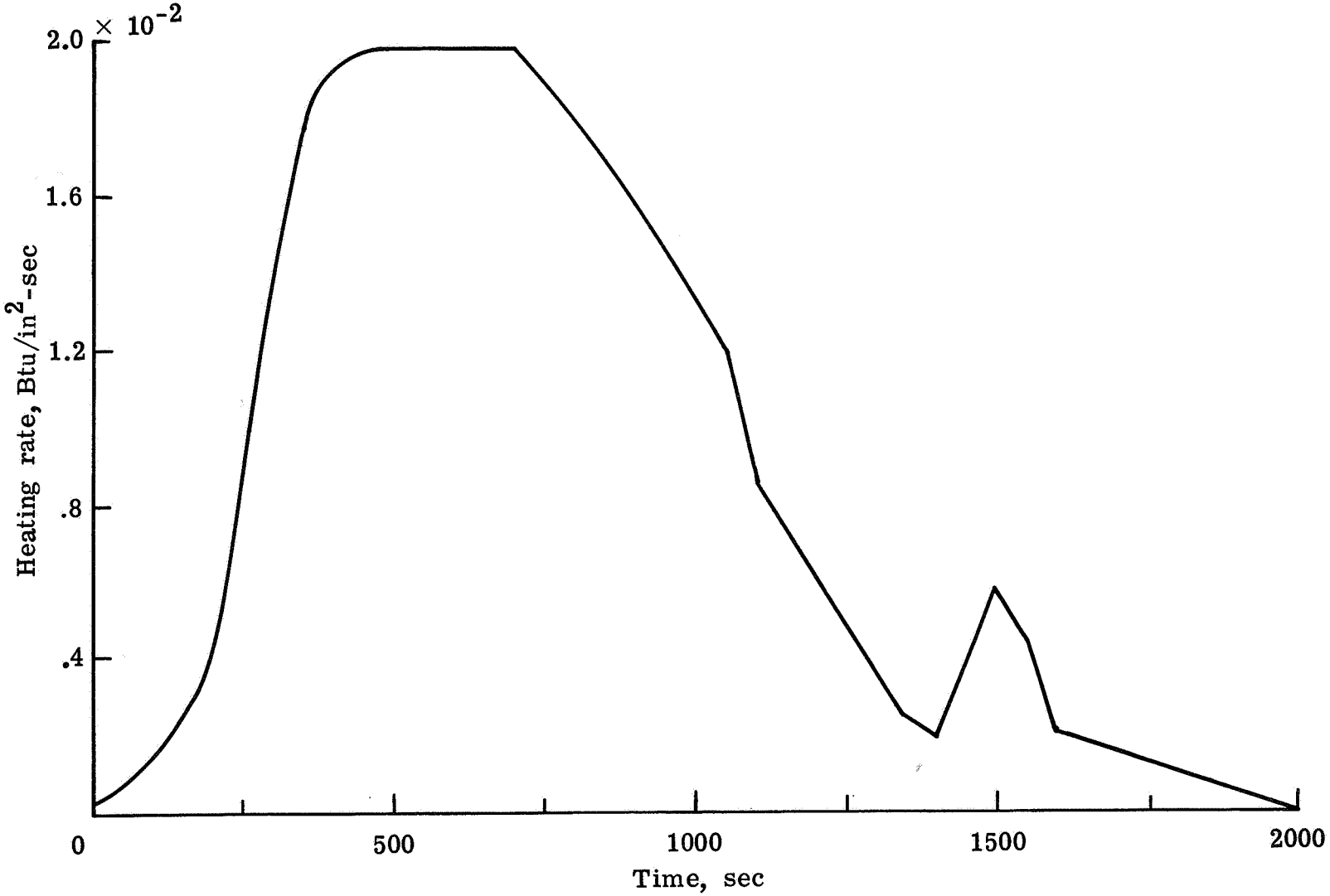

Figure 13.- Heating rate at outer surface of insulated cylinder.

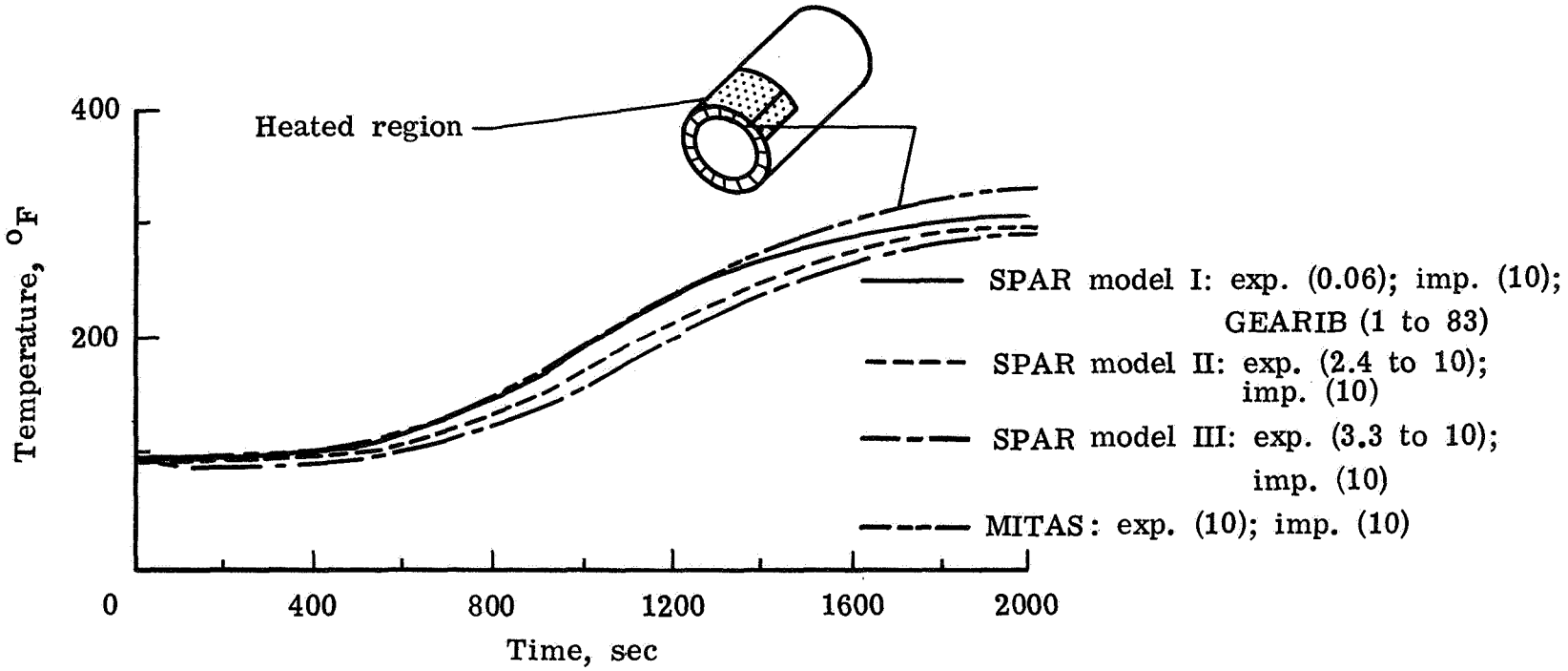

Figure 14.- Effects of algorithm and model on temperature history of insulated cylinder. (Numbers in parentheses are values of DT in seconds.)

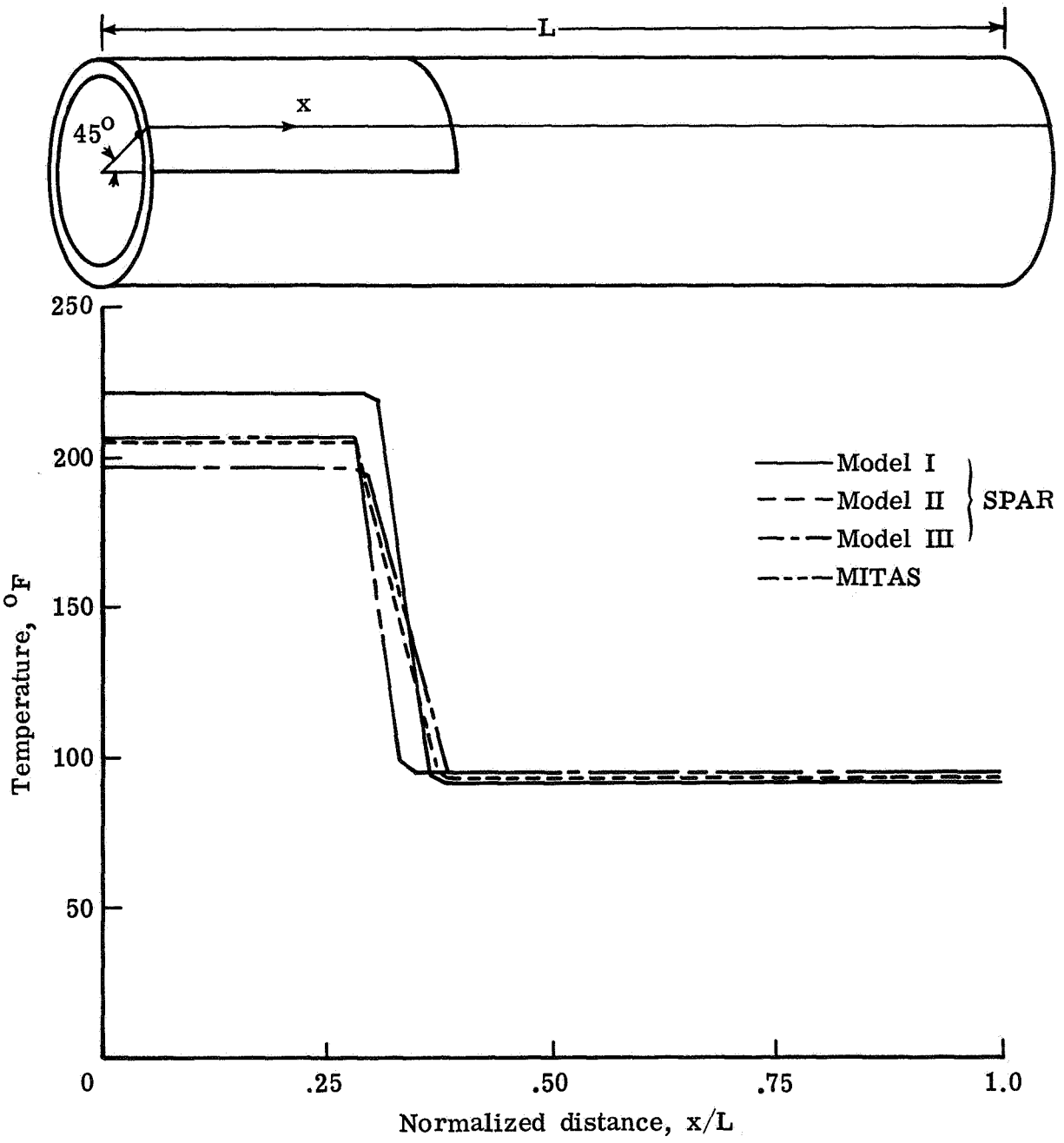

Figure 15.- Effect of models on temperature distribution in insulated cylinder at 1000 seconds.

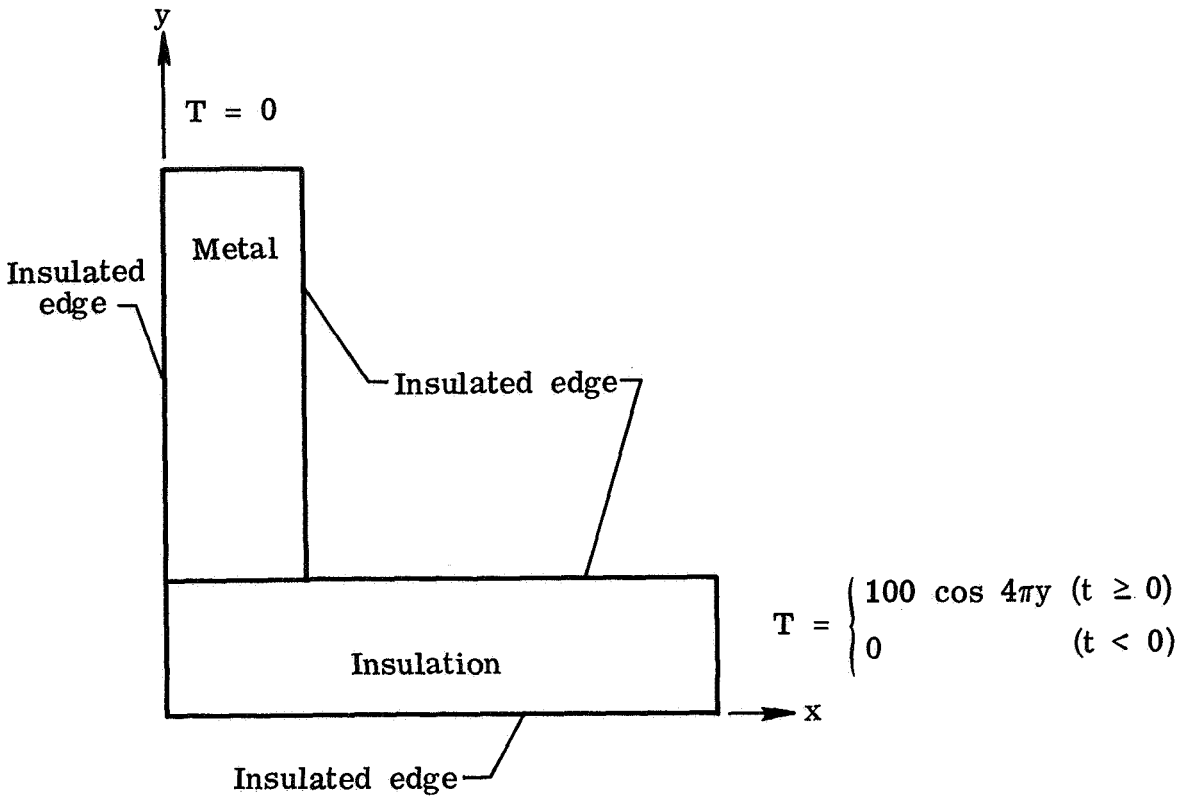

(a) Configuration and boundary conditions.

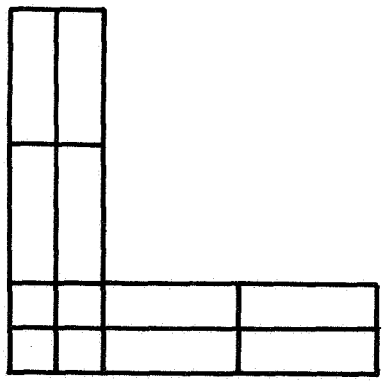

(b) Finite-element model.

Figure 16.- L-shaped insulated metal configuration used to evaluate Hughes-Liu mixed implicit-explicit integration algorithm.

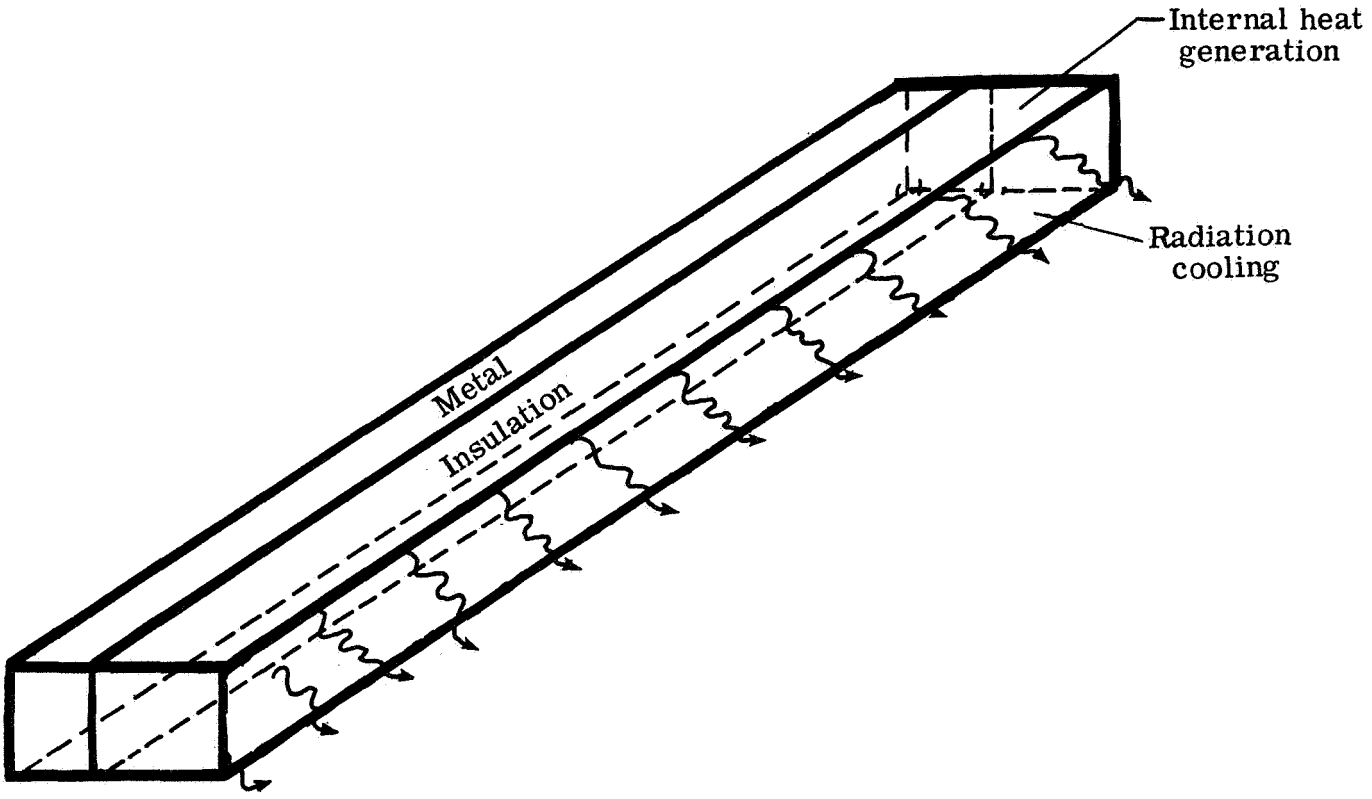

Figure 17.- Insulated slab problem used to assess operator splitting.

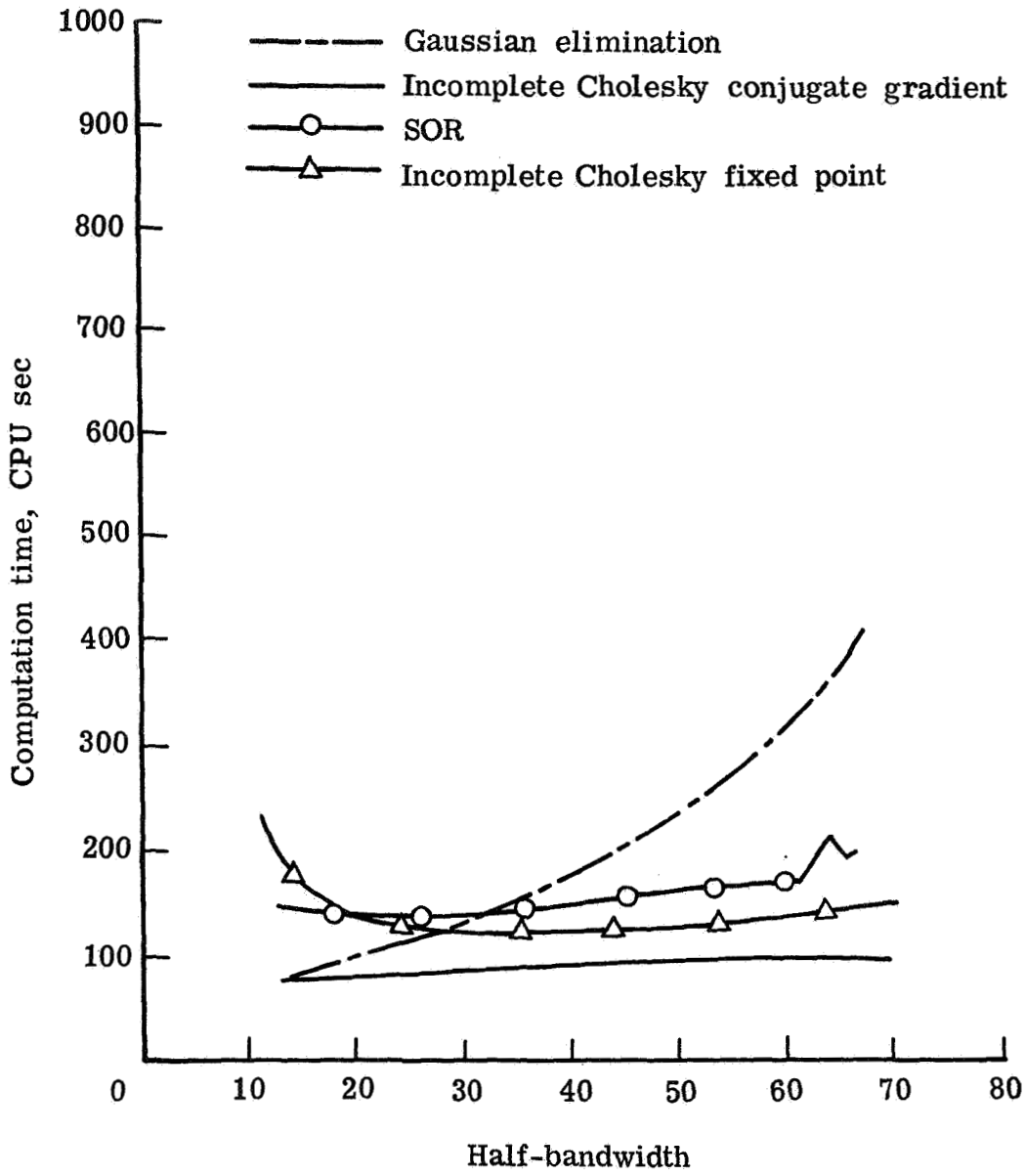

(a) 400 grid points.

Figure 18.- Comparison of various linear operator-splitting techniques in transient thermal analysis of insulated cylinder. (CPU time is for Prime 400 computer.)

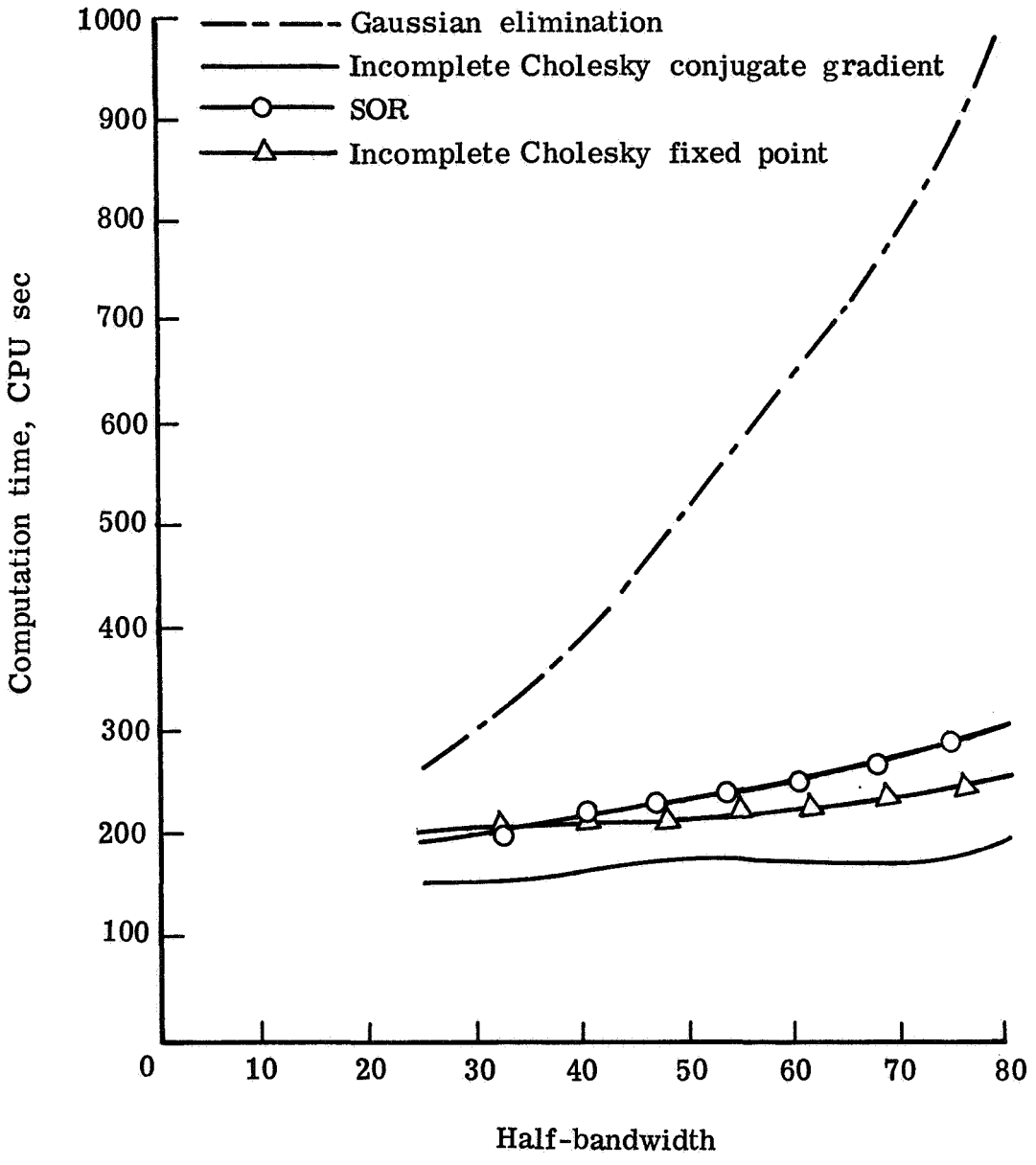

(b) 720 grid points.

Figure 18.- Continued.

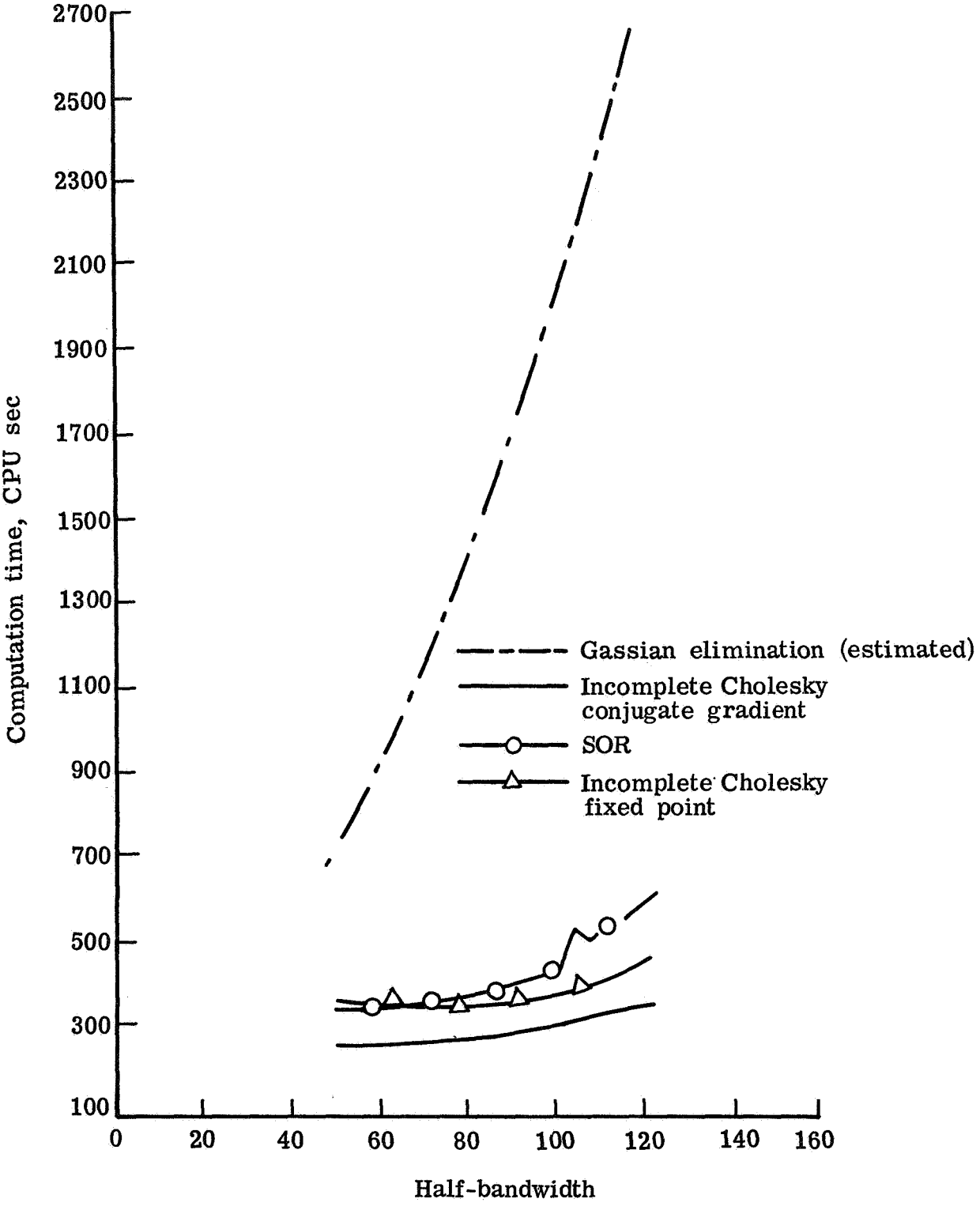

(c) 1100 grid points.

Figure 18.- Concluded.

1. Report No.	2. Government Accession No.	3. Recipient's Catalog No.
NASA TP-2038		

4. Title and Subtitle	5. Report Date
STUDIES OF IMPLICIT AND EXPLICIT SOLUTION TECHNIQUES IN TRANSIENT THERMAL ANALYSIS OF STRUCTURES	August 1982
	6. Performing Organization Code 506-53-53-07

7. Author(s)	8. Performing Organization Report No.
Howard M. Adelman, Raphael T. Haftka, and James C. Robinson	L-15245
	10. Work Unit No.

9. Performing Organization Name and Address	11. Contract or Grant No.
NASA Langley Research Center Hampton, VA 23665	
	13. Type of Report and Period Covered

12. Sponsoring Agency Name and Address	13. Type of Report and Period Covered
National Aeronautics and Space Administration Washington, DC 20546	Technical Paper
	14. Sponsoring Agency Code

15. Supplementary Notes

16. Abstract

Studies aimed at an increase in the efficiency of calculating transient temperature fields in complex aerospace vehicle structures are reported. The advantages and disadvantages of explicit and implicit algorithms are discussed and a promising set of implicit algorithms with variable time steps, known as GEARIB, is described. Test problems, used for evaluating and comparing various algorithms, are discussed and finite-element models of the configurations are described. These problems include a coarse model of the Space Shuttle wing, an insulated frame test article, a metallic panel for a thermal protection system, and detailed models of sections of the Space Shuttle wing. Results generally indicate a preference for implicit over explicit algorithms for transient structural heat-transfer problems when the governing equations are stiff (typical of many practical problems such as insulated metal structures). The effects on algorithm performance of different models of an insulated cylinder are demonstrated. The stiffness of the problem is highly sensitive to modeling details and careful modeling can reduce the stiffness of the equations to the extent that explicit methods may become the best choice. Preliminary applications of a mixed implicit-explicit algorithm and operator-splitting techniques for speeding up the solution of the algebraic equations are also described.

17. Key Words (Suggested by Author(s))	18. Distribution Statement
Transient thermal analysis Numerical integration Insulated structures Finite-element heat transfer	Unclassified - Unlimited Subject Category 34

19. Security Classif. (of this report)	20. Security Classif. (of this page)	21. No. of Pages	22. Price
Unclassified	Unclassified	45	A03

For sale by the National Technical Information Service, Springfield, Virginia 22161

NASA-Langley, 1982

National Aeronautics and
Space Administration

Washington, D.C.
20546

Official Business
Penalty for Private Use, $300

THIRD-CLASS BULK RATE

Postage and Fees Paid
National Aeronautics and
Space Administration
NASA-451

NASA

POSTMASTER: If Undeliverable (Section 158 Postal Manual) Do Not Return